

University of Nebraska - Lincoln

DigitalCommons@University of Nebraska - Lincoln

---

Doctoral Documents from Doctor of Plant  
Health Program

Plant Health Program, Doctor of

---

12-2022

## Image Analysis and Machine Learning in Agricultural Research

Xinzheng Chen

University of Nebraska-Lincoln, xinzheng@huskers.unl.edu

Follow this and additional works at: <https://digitalcommons.unl.edu/planthealthdoc>



Part of the [Agricultural Science Commons](#), [Agriculture Commons](#), and the [Horticulture Commons](#)

---

Chen, Xinzheng, "Image Analysis and Machine Learning in Agricultural Research" (2022). *Doctoral Documents from Doctor of Plant Health Program*. 24.

<https://digitalcommons.unl.edu/planthealthdoc/24>

This Doctoral Document is brought to you for free and open access by the Plant Health Program, Doctor of at DigitalCommons@University of Nebraska - Lincoln. It has been accepted for inclusion in Doctoral Documents from Doctor of Plant Health Program by an authorized administrator of DigitalCommons@University of Nebraska - Lincoln.

IMAGE ANALYSIS AND MACHINE LEARNING IN AGRICULTURAL RESEARCH

by

Xinzheng Chen

A DOCTORAL DOCUMENT

Presented to the Faculty of  
The Graduate College at the University of Nebraska  
In Partial Fulfillment of Requirements  
For the Degree of Doctor of Plant Health

Major: Plant Health

Under the Supervision of Professor Gary L. Hein

Lincoln Nebraska

December, 2022

# IMAGE ANALYSIS AND MACHINE LEARNING IN AGRICULTURAL RESEARCH

Xinzheng Chen, D.P.H.

University of Nebraska, 2022

Advisor: Gary L. Hein

Agricultural research has been a focus for academia and industry to improve human well-being. Given the challenges in water scarcity, global warming, and increased prices of fertilizer, and fossil fuel, improving the efficiency of agricultural research has become even more critical. Data collection by humans presents several challenges including: 1) the subjectiveness and reproducibility when doing the visual evaluation, 2) safety when dealing with high toxicity chemicals or severe weather events, 3) mistakes cannot be avoided, and 4) low efficiency and speed.

Image analysis and machine learning are more versatile and advantageous in evaluating different plant characteristics, and this could help with agricultural data collection. In the first chapter, information related to different types of imaging (e.g., RGB, multi/hyperspectral, and thermal imaging) was explored in detail for its advantages in different agriculture applications. The process of image analysis demonstrated how target features were extracted for analysis including shape, edge, texture, and color. After acquiring features information, machine learning can be used to automatically detect or predict features of interest such as disease severity. In the second chapter, case studies of different agricultural applications were demonstrated including: 1) leaf damage symptoms, 2) stress evaluation, 3) plant growth evaluation, 4) stand/insect counting, and 5) evaluation for produce quality. Case studies showed that the use of image analysis is often more advantageous than visual rating. Advantages of image analysis include

increased objectivity, speed, and more reproducibly reliable results. In the third chapter, machine learning was explored using romaine lettuce images from RD4AG to automatically grade for bolting and compactness (two of the important parameters for lettuce quality). Although the accuracy is at 68.4 and 66.6% respectively, a much larger data base and many improvements are needed to increase the model accuracy and reliability.

With the advancement in cameras, computers with high computing power, and the development of different algorithms, image analysis and machine learning have the potential to replace part of the labor and improve the current data collection procedure in agricultural research.

## ACKNOWLEDGEMENTS

Thanks to my friends and family in China and U.S. that supported me endlessly in my academic endeavors. I would like to thank my committee members Drs. Gary Hein, Sam Wortman, Gerard Adams, and Loren Giesler for their support. Dr. Hein, thank you for welcoming me into the DPH family and guiding me through the program. Kelly White, thank you for your helping me edit the documents. The past nine years at UNL have been a great journey for me to become an agricultural professional. Thank you to my fellow DPH colleagues that went through the tough time with me and gave me moral support.

Grandma, thank you for your high expectation of me by naming me Xinzheng which in Chinese means “new generation with bigger achievement”. You have taught me well to always be a better person.

I would like to dedicate my entire document as a thank you to Research Designed for Agriculture (RD4AG) for providing me with the two internship experiences. Without the help from the company, I would not have gotten this far. As part of the RD4AG family, I would like to name them for their support and great impact in my life. Thanks to Steve West, Lee West, Amy Spencer, Cesar Melendrez, Jesus Urquides, Connor Osgood, Jose Carrillo, Alan Cruz, Léonie Boisleux, Hector Salazar, Luz Salazar, Mario Madrigal, Christian Perez, Oscar Meza, Robert Hill, and Francisco Villegas.

## Table of Contents

<b>Chapter 1: Image analysis to improve data collection in agricultural research .....</b>	<b>1</b>
<b>Introduction.....</b>	<b>1</b>
<b>Imaging.....</b>	<b>3</b>
Image Sensors .....	3
Image Projection.....	4
Electromagnetic Spectrum .....	6
Hyperspectral Imaging.....	7
Multispectral Imaging.....	10
Thermal Imaging .....	11
<b>Digital Image Properties .....</b>	<b>14</b>
<b>Image Acquisition .....</b>	<b>18</b>
Control of the Background.....	18
Control of Lighting Conditions .....	20
Control of Object Features .....	21
<b>Process of Image Analysis .....</b>	<b>21</b>
Image Processing .....	21
Segmentation .....	23
Feature Extraction .....	25
<b>Image Analysis Software .....</b>	<b>28</b>
<b>Image Analysis and Machine Learning.....</b>	<b>29</b>
<b>Challenges of Image Analysis .....</b>	<b>31</b>
<b>Summary.....</b>	<b>32</b>
<b>References .....</b>	<b>34</b>

<b>Chapter 2: Applications using image analysis in applied agricultural research .....</b>	<b>44</b>
<b>Introduction.....</b>	<b>44</b>
<b>Quantifying Leaf Damage Symptoms .....</b>	<b>47</b>
<i>Visual Rating of Leaf Damage .....</i>	47
<i>RGB Imaging for Leaf Damage Estimation .....</i>	49
<i>Using Spectral Sensors for Disease Identification.....</i>	52
<b>Stress Detection Through Imaging Analysis .....</b>	<b>57</b>
<i>Detecting Iron Deficiency with RGB Imaging.....</i>	57
<i>Drought Stress Detection .....</i>	59
<i>Salt Stress Detection.....</i>	62
<b>Plant Growth (Vigor) Evaluation .....</b>	<b>64</b>
<i>RGB Imaging.....</i>	64
<i>Spectroradiometer Imaging .....</i>	66
<b>Image Analysis for Counting.....</b>	<b>67</b>
<i>Insect Counting .....</i>	68
<i>Insect Counting Using Machine Learning .....</i>	70
<i>Plant Stands Counts .....</i>	73
<b>Quality and Size Evaluation .....</b>	<b>74</b>
<i>Surface Defect Detection and Grading .....</i>	75
<i>Sorting for Maturity and Size .....</i>	77
<b>Summary.....</b>	<b>79</b>
<b>References .....</b>	<b>81</b>
<b>Chapter 3: Machine learning grading for lettuce bolting and compactness .....</b>	<b>90</b>

<i>Introduction</i> .....	90
<i>Materials and Method</i> .....	93
<i>Results and Discussion</i> .....	94
.....	97
<i>References</i> .....	101

## **Chapter 1: Image analysis to improve data collection in agricultural research**

### **Introduction**

Agricultural research has been a focus for academia and industry with a targeted goal of improving human well-being. As the world population continues to increase, approximately 80% of the population will be living in urban areas with an even higher demand for food (Kalantari et al. 2017). The rapidly growing population also intensifies competition and exploitation of land, water, and other natural resources (Gupta et al. 2020). Given the challenges, such as water scarcity (Mancosu et al. 2015) and global warming (Cline 2008), improving the efficiency of agricultural research has become even more critical. Researchers consider experimental design, planting, applications, data collection, data analysis, and report writing. The processes of experimental design, planting, and applications have been greatly improved with advanced software, high-tech planters, and sprayer technology. However, data collection is often the least developed and most labor intensive. This is partly due to agricultural research dealing with diverse crops and growing conditions. In addition, testing different chemicals such as herbicides, pesticides, fungicides, and growth regulators requires measuring very different parameters.

Data collecting in agricultural field research presents several challenges. First, humans are subjective when visually evaluating severity such as pest damage, disease infection, or herbicide efficacy. Even with proper training, raters can still be biased, and data collected might not be representative of the actual treatment. Koch and Hau (1980) demonstrated individuals can be biased to a preferred value when doing disease severity assessment. Accurate measurement of disease severity is important in making decisions

for treatment, disease forecasting, estimating yield loss, and for evaluating disease resistance in variety development (Bock et al. 2020). Inaccuracies can sabotage the research process, change research direction, and impact grower profitability. Bock et al. (2009) assessed citrus canker foliar symptoms by comparing 28 human raters (experienced and inexperienced) with standardized image analysis using 200 digital leaf images that ranged from 0 to 37% infected area. Lesion number, percent necrotic area (%N), and total percent chlorotic + necrotic area (%CN) were measured. Results showed that raters were biased and tend to overestimate %N and %CN when the range is over 8%. Thus, estimates of leaves with greater lesion numbers will result in an overestimation of %N and %CN. Bock et al. (2009) also showed that some raters were innately more accurate than others.

Another challenge involves the safety associated with data collection. Humans are fragile when exposed to extreme environmental conditions and toxic agricultural chemicals. Sending researchers to collect data in these situations can put them in potential danger or make them uncomfortable. For example, organophosphates are pesticides widely used in agriculture to protect crops. Exposure to organophosphates could induce cardiovascular, reproductive, and nervous system effects (Hung et al. 2015, Miranda-Contreras et al. 2013, Rosenstock et al. 1991, Wesseling et al. 2002).

A challenge that impacts data quality and efficiency relates to the fact that humans are fallible and can have limited attention spans. When collecting data, through boredom or distraction, mistakes cannot be avoided all the time. The fallibility and errors made by researcher are well documented by Kovacs et al. (2021). Common errors include accidentally overwriting data, recording data incorrectly (e.g., making typos), and

incorrectly copying and pasting data sets. In addition, after long hours of scoring plants fatigue can impact the quality of data. These factors can lead to large intra-rater variability in rating scores, thus resulting in reduced accuracy and reproducibility (Naik et al. 2017).

Finally, human evaluation and data collection can be slow. Sending researchers to collect data can be time consuming. Chung et al. (2016) studied the accurate detection of *Fusarium fujikuroi* for two rice cultivars. Because the symptoms of this disease are complex and vary with the cultivar, accurate identification of infected plants by visual inspection is difficult and time consuming. Chung et al. (2016) used image analysis and machine learning for disease detection. They showed these methods to be faster and more effective, and they were able to distinguish infected and healthy seedlings with an accuracy of 87.9% using image analysis and positive prediction at 91.8% using machine learning.

To address these challenges, image analysis could be one solution to help researchers with these data collecting challenges. This chapter provides fundamental information on using imaging, spectral properties, and image analysis to improve the quality and efficiency of collecting agricultural data in the field.

## **Imaging**

### *Image Sensors*

When visible light strikes an object, it is either absorbed, reflected, or transmitted according to the light property and the nature of the material (Manickavasagan and Jayasuriya 2014). If visible light is reflected from an object, a digital camera can receive

that light and convert the light into electrical signals (Gómez-López and Bhat 2021). These electrical signals are proportional to the light intensity and translated into digitized data that are stored in the computer as a digital image. Imaging involves acquiring spatial and temporal data from an object (Garini et al. 2006). Visible light images are the most common images used for image analysis.

Digital cameras will contain one of two main types of light sensors, charge-coupled device (CCD) or complementary metal oxide semiconductor (CMOS). Both CCD and CMOS cameras are silicon-based and use the photoelectric effect to create electrical signals from light. CCD sensors use a linear array configuration while CMOS sensors use a multiple array configuration (Gómez-López and Bhat 2021). In CCD sensors, every pixel's charge is transferred to a single output node to be converted to voltage, buffered, and sent off chip as an analog signal (Sonka et al. 2014). CCD sensors have the advantage of producing a clearer picture but has higher battery consumption, and the single output node often results in overheating. In CMOS sensors, each pixel has its own charge-to-voltage conversion. With each pixel doing its own conversion, uniformity is lower, but it is also massively parallel, allowing for higher total bandwidth and speed (Sonka et al. 2014).

### *Image Projection*

An image is a projection of a three-dimensional scene into a two-dimensional projection plane. The illumination source can be sunlight or other light sources, and the amount of incident illumination can be represented as  $i(x, y)$ . The amount of illumination reflected by the scene element can be represented as  $r(x, y)$ . Then, the image captured by

the sensor is expressed as a continuous function of two coordinates in the projection plane:  $f(x, y) = i(x, y) * r(x, y)$  (Figure 1.1) (Mishra et al. 2017). In each position  $(x, y)$  in the projection plane,  $f(x, y)$  is the light intensity at this point. During the digitization process, the function  $f(x, y)$  is sampled into a matrix with  $M$  rows and  $N$  columns also known as spatial sampling (Balter 1993). The smallest sampling point in the grid corresponds to picture element or pixel in the digital image. The pixel is the smallest observable unit in the image. Every pixel in an image has a coordinate  $x/y$  or  $i/j$  that identifies its location within the image grid creating the spatial layout of an image. For example, in Figure 1.2, the green pixel in the example has the coordinate of  $(1,0)$ , the yellow pixel has the coordinate of  $(4,2)$ , and the white pixel has the coordinate of  $(2,3)$ .

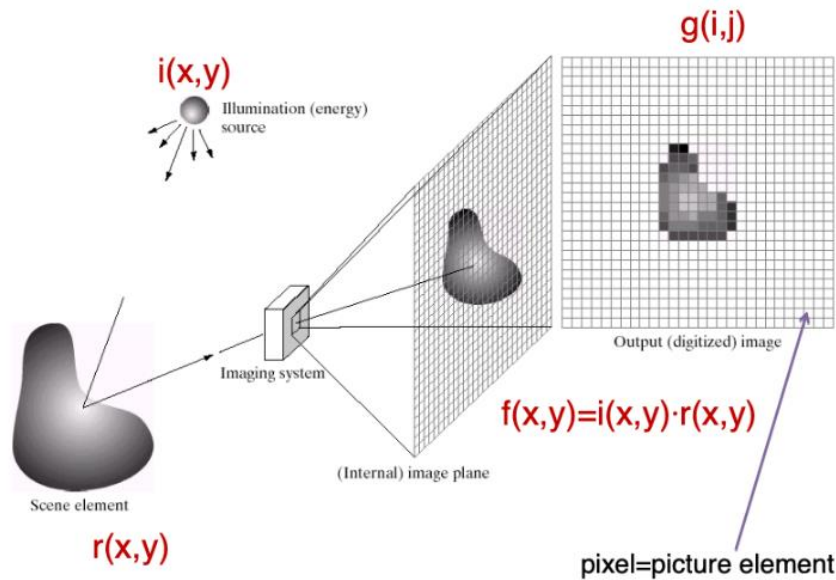


**Figure 1.1.** The process of image projection of a three dimensional scene onto a two dimensional projection plane (figure modified from Mishra et al. 2017).

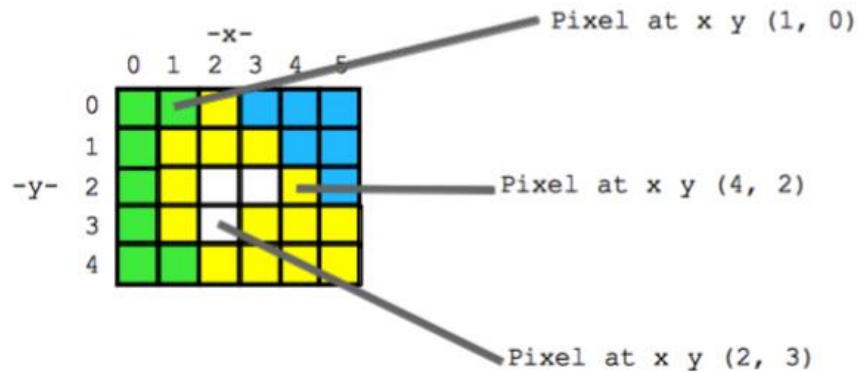


**Figure 1.2.** Pixel coordinates in the two-dimensional matrix (figure source: <https://web.stanford.edu/class/cs101/image-1-introduction.html>).

### *Electromagnetic Spectrum*

Different types of imaging can be used for specific purposes. To evaluate the various applications of imaging, it is important to understand the basics of the electromagnetic spectrum.

The electromagnetic spectrum consists of different electromagnetic radiation, which by definition is “a form of oscillating electrical and magnetic energy capable of traversing space without benefit of physical interconnections” (Herter 1985). As electromagnetic radiation passes through space, the distribution of the radiant energy forms the electromagnetic spectrum. Electromagnetic radiation behaves as waves with the properties of wavelength ( $\lambda$ ) and frequency ( $\nu$ ). A shorter wavelength with higher frequency possesses higher energy but travel shorter distances (e.g., x-ray). A longer wavelength with lower frequency possesses lower energy but will travel longer distances (e.g., radio waves). The most relevant wavelengths for imaging fall in the visible spectrum and beyond to include the near-red and infrared wavelengths. The human eye can detect the visible light range from 400-700 nm in wavelength, and this is fundamental

to visible light imaging. This visible region is found between the ultraviolet (100-400 nm) and infrared regions (700-1000 nm) (Figure 1.3).

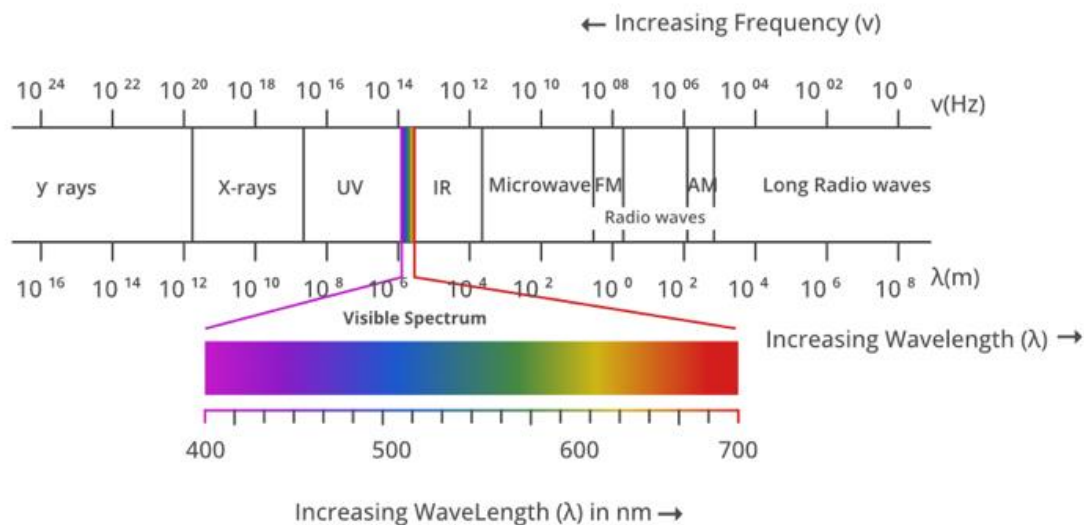


**Figure 1.3.** Electromagnetic spectrum showing the visible spectrum from 400-700 nm in wavelength (figure source: <https://www.geeksforgeeks.org/electromagnetic-spectrum/>).

### *Hyperspectral Imaging*

Hyperspectral imaging has been used extensively in remote sensing and widely explored by NASA for geophysical research (Goetz 2009). Hyperspectral imaging technology can engage with reflected, transmitted, emitted, and diffusely scattered light (Wieme et al. 2022). It provides a continuous measure of the electromagnetic radiation across a wide range of wavelengths, typically in the wavelength range of 400–2500 nm (Wieme et al. 2022). The wavelengths measured are continuous and contiguous with a narrow bandwidth (typically below 10nm). This enables detection of subtle changes in biochemical and biophysical attributes of the crop plants and their different physiological processes (Sahoo et al. 2015). Hyperspectral imaging is the integration of conventional imaging and spectroscopy (Gowen et al. 2007). For a hyperspectral camera, conventional

imaging captures the spatial information at every pixel of the image,  $I(x,y)$ , and the spectrometer provides the spectral information at each pixel  $I(\lambda)$ . Combined, the spectral image is described as  $I(x,y,\lambda)$  as a hypercube (Figure 1.4). It can be viewed as an image  $I(x,y)$  at each wavelength  $\lambda$ , or as a spectrum  $I(\lambda)$  at every pixel  $(x,y)$  (Garini et al. 2006).

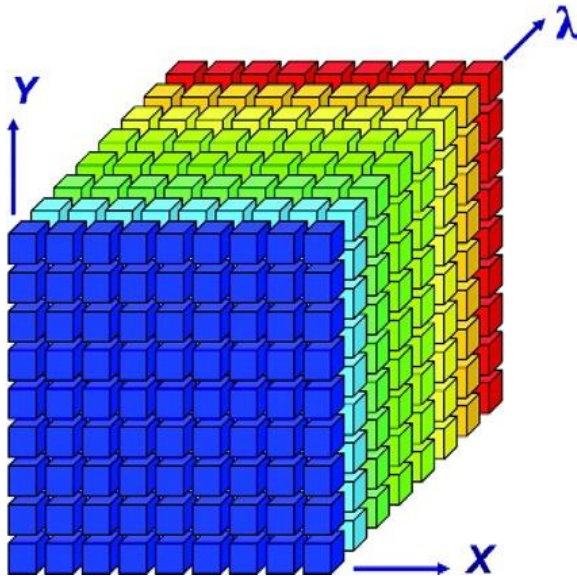


**Figure 1.4.** Spectral image data represented as a data cube (figure source Garini et al. 2006).

At each wavelength the image data provides the spatial distribution of the spectral intensity. This wealth of data collected enables one to analyze samples more comprehensively (Long et al. 2023). Hyperspectral imaging has demonstrated a wide range of uses in agriculture. Some of these include: predicting yield (Pradhan et al. 2014, Wang et al. 2008), measuring chlorophyll content (Gao et al. 2021, Ji-Yong et al. 2012), predicting nitrogen use efficiency (Olson et al. 2022, Wang et al. 2019), detecting and measuring disease (Bock et al. 2010, Lowe et al. 2017, Moghadam et al. 2017), and water stress (Kim et al. 2015, 2011). However, due to the extensive amount of spatial and

spectral data, these data inevitably contain noise and redundant information (Long et al. 2023). Several classification or regression analysis methods have been used to handle the data, such as principal component analysis, partial least squares discriminant analysis, support vector machine, artificial neural network, radial basis function network, and k-nearest neighbors (Long et al. 2023).

Hyperspectral imaging has been widely used in food safety for assessment of fungal damage. Shahin and Symons (2011) used hyperspectral imaging in the visible-NIR (400-1000nm) wavelength range to detect *Fusarium*-damaged wheat kernels. In this range, *Fusarium*-damaged kernels have higher reflectance because of the white or pinkish fungal tissue on the kernel surface. Peiris et al. (2009) found short wavelength infrared (SWIR) at 1000-1700nm was good at detecting changes in moisture, carbohydrate, and protein content in wheat kernels. *Fusarium*-damaged wheat kernels contain less water, carbohydrates, and proteins which are easy to separate by wavelength. Hyperspectral imaging has also been implemented in measuring vegetable and fruit maturity, firmness, soluble content, inner bruises etc. (Gómez-López and Bhat 2021).

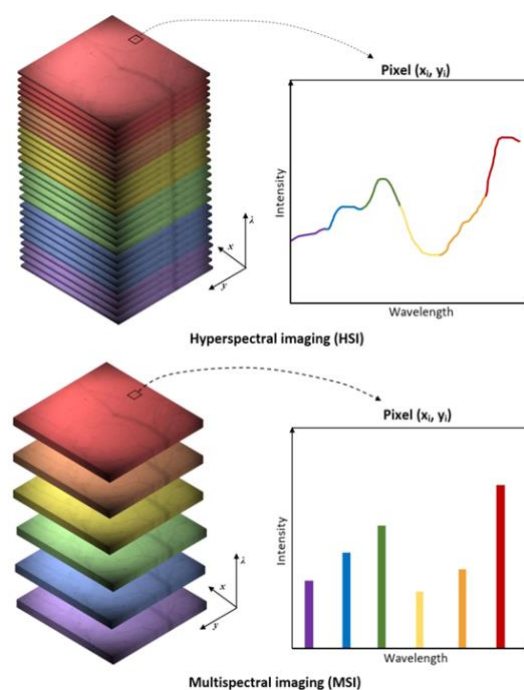


**Figure 1.5.** Differences between hyperspectral and multispectral imaging (figure source Giannoni et al. 2018).

### *Multispectral Imaging*

Multispectral imaging is facilitated by collecting spectral signals at a few discrete bands, each spanning a broader spectral range from tens to hundreds of nanometers (Lu et al. 2020). The differences between hyperspectral and multispectral imaging are illustrated in Figure 1.5 (Giannoni et al. 2018). Multispectral imaging generally measures a few distinct spectral channels, often in the red, blue, green, near infrared (NIR), short-wave infrared (SWIR), or infrared (IR) wavelengths. Since multispectral imaging does not measure contiguous spectral bands, researchers are limited to evaluating differences in a small number of the positions in the wavelength range (Lowe et al. 2017).

To be most useful, the wavelengths included in the multispectral cameras should represent key areas on the electromagnetic spectrum. One example that uses strategic wavelengths would be to determine the Normalized Difference Vegetation Index (NDVI). NDVI is commonly used to measure the health of vegetation. Healthy vegetation contains more chlorophyll which absorbs red and blue light and reflects near infrared (NIR) and green light. Calculation of NDVI uses measurements from red (660 nm) and NIR (770 nm) wavelengths in the following formula:

$$NDVI = \frac{(NIR - RED)}{(NIR + RED)}$$

A large number of indices have been established that provide diverse measures of reflectance characteristics. Another index used in monitoring plant health is the photochemical reflectance index (PRI). This index estimates the ratio of carotenoid to chlorophyll that can aid in estimating photosynthetic light use efficiency by using the increase in green reflectance at the wavelength around 550nm (Gamon et al. 1992). PRI (Sims and Gamon 2002) is estimated using the formula:

$$PRI = (R_{531} - R_{570}) \times (R_{531} + R_{570})$$

One common index used for leaf rust disease severity (LRDSI) was developed by Ashourloo et al. (2014) that has shown accuracy of 89% in detecting the disease. The formula requires the measurement of wavelength  $R_{605}$  and  $R_{455}$ :

$$LRDSI = 6.9 \times \frac{R_{605}}{R_{455}} - 1.2$$

Another common index focuses on changes in the sudden increase in reflectance at the red and near infrared border. The ‘red edge’ is the bandwidth from 690-740nm where the visible spectrum ends, and the near infrared starts. This region shows a large change in spectral response for green plant materials because chlorophyll strongly absorbs wavelengths up to around 700 nm (Lowe et al. 2017). Study by Fernández et al. (2020) showed the red and red-edge spectral region can help detecting potato late blight at the leaf and canopy levels.

### *Thermal Imaging*

Thermal imaging is a branch of remote sensing dealing with acquisition, processing, and interpretation of data acquired primarily in the thermal infrared (TIR) region of the electromagnetic spectrum (Ishimwe et al. 2014). Remote sensing in the thermal infrared range measures radiation emitted from the subject. The thermal infrared region covers wavelengths from 3 to 35  $\mu\text{m}$ . Wavelengths from 3-5  $\mu\text{m}$  overlap with solar reflection, and wavelengths from 17-25  $\mu\text{m}$  are still not well researched (Ishimwe et al. 2014). Thus, wavelengths from 8-14  $\mu\text{m}$  have been used in thermal remote sensing since it is the most representative and least affected by atmospheric absorption (Kant et al. 2009). Infrared thermal imaging can be applied in the field where there are

temperature differences. In agriculture, thermal imaging can be used to predict water stress in crops (Cohen et al. 2012), irrigation scheduling (Roopaei et al. 2017), disease detection such as citrus greening (Sankaran et al. 2013), detection of serious pests such as red palm weevils (Ahmed et al. 2019, Golomb et al. 2015), predicting yield (Elsayed et al. 2017, Pradawet et al. 2022), and bruise detection in fruits and vegetables (Ishimwe et al. 2014). As plants are heated by radiation, they transpire to prevent overheating. If plants do not have enough water or heating exceeds the transpiration rate, plants are water stressed (Kacira et al. 2005) and their temperature becomes elevated.

The empirical crop water stress index (CWSI) is used to measure plant water stress (Idso et al. 1981) by using the differences between foliage or canopy temperature ( $T_c$ ) and air ( $T_a$ ) temperature and vapor pressure deficit (kPa) (Figure 1.6). Depending on the specific cultural condition and crop, an upper and lower limit needs to be established. The upper limit ( $T_c - T_a$ ) is established using data collected from severely stressed plants. The lower limit (non-water stressed baseline), ( $T_c - T_a$ ) is collected from well-watered plants.

$$CWSI = \frac{(T_c - T_a) - (T_c - T_a)_{lower\ limit}}{(T_c - T_a)_{upper\ limit} - (T_c - T_a)_{lower\ limit}} = \frac{BA}{CA}$$

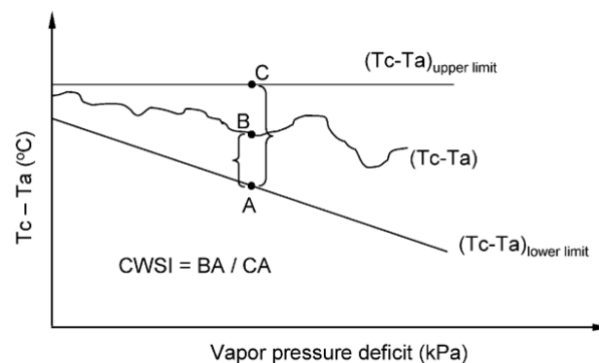


**Figure 1.6.** Empirical demonstration of the calculation of crop water stress index (CWSI) (figure source Kacira et al. 2005).

The values for CWSI range from 0 to 1. Values close to 0 represent plants that are well watered, and values close to 1 represent severely stressed plants (Kacira et al. 2005).

For disease detection using thermal imaging, temperature is generally negatively correlated with transpiration rate (Lindenthal et al. 2005). Diseased plants will increase stomatal closure, and this often leads to decreased transpiration rate and increased leaf temperature. Lindenthal et al. (2005) used digital infrared thermography to image downy mildew (*Pseudoperonospora cubensis*) infection on cucumber leaves. They found that leaf temperature during downy mildew development of infected leaves were considerably higher than the healthy ones. The maximum temperature difference within a thermogram of cucumber leaves allowed the discrimination between healthy and infected leaves before visible symptoms appeared (Lindenthal et al. 2005). Other pathogens have also shown increases in temperature during infection. This includes thermal imaging of tobacco plants infested with tobacco mosaic virus (Chaerle et al. 1999, 2001). Surprisingly, some pathogens can suppress stomatal closure resulting in decreased temperature compared with healthy plant. For example, the fungus, *Cercospora beticola*, infested on tobacco plants caused decrease in temperature (Chaerle et al. 2004). Bacterial pathogens, such as *P. syringae* and *Xanthomonas campestris* pv. *campestris* also suppressed stomatal closure at early stages of infection to promote entry into leaf tissue (Bunster et al. 1989, Gudesblat et al. 2009). Thus, thermal imaging has great potential to identify different types of plant disease, but temperature changes can be pathogen specific on different plants (Mutka and Bart 2015).

## Digital Image Properties

Digital images include color (intensity) information. The simplest example would be binary images where there are only two colors, and each color is represented by one number (0 for black and 1 for white). Bit depth refers to the color information stored in an image. Typically, the bit depth is used to determine the color of a single pixel in an image (Gómez-López and Bhat 2021). For example, 8 bit is  $2^8$  or 256 colors, and 16 bit is  $2^{16}$  or 65536 colors. One bit would be the lowest color (binary image) which is  $2^1$  (2 colors: black and white). Grayscale range in color from black (0) to white (at maximum of 255) according to the signal level. As the bit depth increases, the greater the color options. Also, as the bit depth increases, the file size of the image also increases because more color information has to be stored for each pixel in the image.

Spatial resolution is determined by density of the pixels and the optical resolution of the camera used to capture the image. The optical resolution is dependent on sampling frequency or number of pixels utilized to construct a digital image. This quantity is dependent upon how finely the image is sampled during acquisition or digitization, and it is highly dependent on the hardware capability of the camera (Davidson 2016). Image brightness (or luminous brightness) is a measure of intensity after the image has been acquired with a digital camera or digitized by an analog-to-digital converter.

A color model is a method to specify and visualize color numerically in digital images. Depending on the type of the image processing applications, researchers require to select proper color spaces (Asmare et al. 2009). Each color model has advantages for analyzing specific types of images. Common color models include RGB (red, green,

blue), CMY (cyan, magenta, yellow), HSI (hue, saturation, intensity), and  $L^*a^*b^*$  (lightness, red/green value, blue/yellow value).

The RGB model is an additive color model that uses transmitted light to display colors (Yam and Papadakis 2004). Three primary colors channels (red, green, and blue) are used per pixel with various intensity values for each (range from 0 to 255). Figure 1.7 illustrates examples of the proportion and intensity for each pixel. This model is commonly used for televisions, computer screens, digital cameras, and scanners that produce colored pixels by red, green, and blue electron guns which “bombard” the phosphorus pixels (Dwairi et al. 2010). The RGB color model is similar to how humans perceive color in the retina (Yam and Papadakis 2004).

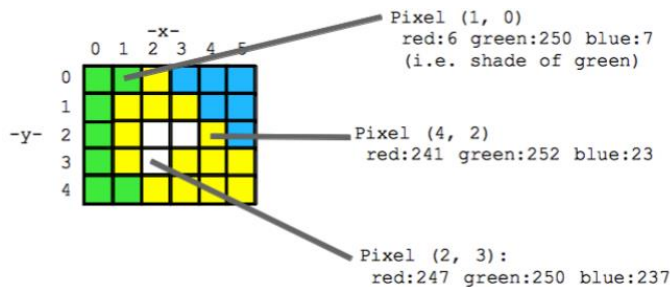


**Figure 1.7.** Pixel coordinates and RGB intensity values for the RGB color model (figure source: <https://web.stanford.edu/class/cs101/image-1-introduction.html>).

The CMY model is subtractive and device dependent which cyan, magenta, and yellow inks are applied to a white surface and subtracts some color from the white surface and create the final color (Kour 2015). This model is mostly used in painting/printing (Dwairi et al. 2010). The color components cyan, magenta, and yellow each have values in the range from 0 to 255 like in RGB imaging (Kour 2015). According to the CMY model, equal amounts of cyan, magenta, and yellow ink should

produce black. However, this process can result in over consumption and the black color created is not pure (Mete and Topaloglu 2009). Because of that, the fourth color component K is added. K represents the color black and has a range from 0 to 1 (0 is no and 1 is yes). In this case, the new model is called the CMYK model.

The HSI model is the improved version of RGB model because it is user oriented (Kour 2015). The components for the HSI model are hue, saturation, and brightness. Hue defines the color itself. Hue is attributed with the dominant wavelength in a mixture of light waves where the dominant color is perceived by an observer (Dwairi et al. 2010). Values for the hue axis vary from 0 to 360 degrees. Saturation represents the amount of color diluted with white light. This model separates the luminance component from the chrominance component. The chrominance component depends on how humans perceive this color spectrum (Kour 2015). In the HSI model, the S varies from 0 to 1 and Intensity varies from 0 (black) to 1 (white) (Kour 2015).

The L\*a\*b\* model is an international standard for color measurement developed by the Commission Internationale d'Eclairage (CIE) in 1976 (Yam and Papadakis 2004). The L\*a\*b\* model consists of a luminance or lightness component (L\* range from 0 to 100) along with two chromatic components (a\* and b\* both range from -120 to +120) (Yam and Papadakis 2004). The a\* component ranges from color green to red and the b\* component ranges from blue to yellow. The L\*a\*b\* model is device independent and provides consistent color regardless of the input or output device such as digital camera or scanner (Yam and Papadakis 2004). Each of these models has an algorithm used in image processing applications (Ibraheem et al. 2012).

Image formats are generally separated based on their status as compressed and uncompressed images. The most common compressed image is the Joint Photographic Experts Group (JPEG) image, and the most common uncompressed image is the Tagged Image File Format (TIFF) image. Image compression includes lossy and lossless compression. Lossy compression creates smaller files by discarding excess image data from the original image. The excess image data removed includes details that are too small for the human eye to differentiate, but it retains its close approximation to the original image (Morkel et al. 2005). JPEG images undergo lossy compression, and repeated use and re-saving can severely deteriorate the image quality. Lossless compression images never remove any information from the original image, but they represent the data in mathematical formulas (Morkel et al. 2005). Thus, the integrity of the original image is maintained, and decompressed images are bit-by-bit identical to the original image input. Graphical Interchange Format (GIF) and 8-bit BMP (Windows bitmap file) are the examples of the lossless compression.

TIFF images are well-known uncompressed images. This is because TIFF files include multiple “chunks” of data called “tags” which convey the image information. The 70 different tag types in the TIFF file ensure the level of complexity and allows great flexibility between viewings (Wiggins et al. 2000). For image analysis, saving as a TIFF is the safe and wise choice because this is a lossless format, and all data are preserved. TIFF can support the full range of image sizes, resolutions, and color depths (Wiggins et al. 2000). File sizes change based on the format used to save images, and this might be an issue when processing images on computers with lower RAM. Typically, saving as a TIFF will have bigger file size compared to saving as a JPEG. For example, the file size

of a TIFF at pixel dimension of 320 X 240 at 24- BIT is about 10 times higher than saving as a JPEG.

For most digital cameras, GPS coordinates are now automatically captured when a picture is taken. The GPS location can be very useful when mapping the picture into the research plot area by using remote sensing software like QGIS or ArcGIS. In agricultural research, GPS can be used for pest and disease scouting, yield mapping, field boundary mapping, soil sampling and property mapping, and weeds and pests mapping (Shamshiri 2009). This can be beneficial for researchers to locate where the picture was taken and assign it to a plot or specific research site.

### **Image Acquisition**

The quality of the picture is the most important part in approaching image analysis. The desired detail in an image may be impossible to identify if image quality is too low. Examples of this include over exposure, excess shadows, distracting debris, or depth of field and focusing issues. High quality images can decrease the time taken for image processing and reduce the complexity in the image processing steps (Vithu and Moses 2016). Following are several considerations for capturing quality images. These are based on the personal experience at Research Designed for Agriculture (RD4AG, Yuma, AZ) when doing image analysis of field acquired images.

#### *Control of the Background*

Color contrast is important when selecting backgrounds. For example, when taking pictures of green plants, it is much easier to use black as a background. However, excessive light reflection from black backgrounds might show more as blue and make it

difficult to segment out these areas in image analysis. Using a pink background was found to be easier since it is rare to see pink in plants, especially in vegetable fields. In addition, it is important to keep the background clean because dust, dirt, and plant debris can create noise in the image analysis process. Another issue in controlling image quality is to establish methods to maintain the consistency of the image framing. This is particularly important when comparing images from plot to plot or from sampling time to sampling time. Using a selfie stick set at a consistent height enables taking repeat images at the same height. Before taking the first image set, mark the spot at each plot to ensure the image will be taken at the same spot throughout the growing season (Figure 1.8).



**Figure 1.8.** Using a selfie stick with the camera mounted will ensure taking images at the same height (image by Xinzheng Chen).

### *Control of Lighting Conditions*

Use of natural or supplemental lighting can be critical for taking quality pictures. For example, taking pictures early or late in the day might reduce the brightness of the image making it easy to separate the plant from the background in the image analysis process. Depending on the light angle, shadows from the photographer or the equipment can be an issue as well. To address this difficulty, a mobile image cart with the camera mounted on top to control the distance and a shade cloth to provide shade and uniform lighting can be used (Figure 1.9).



**Figure 1.9.** Using a mobile cart to take images in the field. Taking images for Downy Mildew evaluation on melon leaves (left). Images for quality evaluation of iceberg lettuce for compactness (right). Note camera is mounted to control distance and shade cloth for controlled lighting (image by Xinzheng Chen).

One problem of using the mobile cart with a camera mounted on top with a clicker is the difficulty in previewing the picture. If focus or framing issues are not noticed in the field, valuable sampling images may be unusable. Connecting a small preview screen to the side of the cart can be an improvement for real time monitoring of the image quality.

### *Control of Object Features*

When doing destructive sampling (e.g., leaf sampling for disease or pest infestation) taking images of the sampled leaves can be challenging. Leaves are not completely flat, and this unevenness can be an issue in lighting, exposure, and focus of the entire leaf. Using non-glare glasses to hold down the leaves can be a better solution.

### **Process of Image Analysis**

General processes for image analysis include image acquisition, processing, segmentation, and feature extraction (Grande 2012, Klukas et al. 2014). As discussed previously, image acquisition is the process of acquiring digital images. The mechanism converts the reflected light from an object to electrical signals and digitizes the image. During this process, controlling background, lighting conditions, and object features are important to ensure the image quality.

### ***Image Processing***

Image processing is the process of denoising or using filters to increase sharpness and highlight the image features. It is critical so that useful information can be obtained from the image by having sufficient contrast between the image features and the background (Grande 2012). The image histogram is a bar chart that graphically represents the shades of tone that make up the digital photograph (Evening 2007). An image histogram is produced by recording the number of pixels at a particular shade of gray. A basic grayscale uses 256 shades of gray to describe all the shades from black (0 value) to white (255 value). Figure 1.10 is an example of grayscale for iceberg lettuce. Histogram manipulation can improve the contrast between the image features and the background by equalization (Figure 1.11). This operation stretches dense parts of the

histogram, where contrast is low and condenses sparse parts of the histogram, where contrast is high (Łabędź et al. 2021). If the histogram shows a bias toward the lower intensity gray levels, then transformation to achieve a more equitable sharing of pixels among the gray levels would enhance or alter the appearance of the image (Awcock and Thomas 1995). This can be done by stretching or compressing gray levels without any alteration in the structural information in the image (Awcock and Thomas 1995).

If an image has insufficient information for extracting the image features, brightness of the image can be altered. Brightness can be adjusted by adding or subtracting a certain value to the gray level of each pixel (Sinecen 2016). Contrast of an image can be changed by multiplying pixel gray values by a certain amount in certain ranges of the histogram (Sinecen 2016).

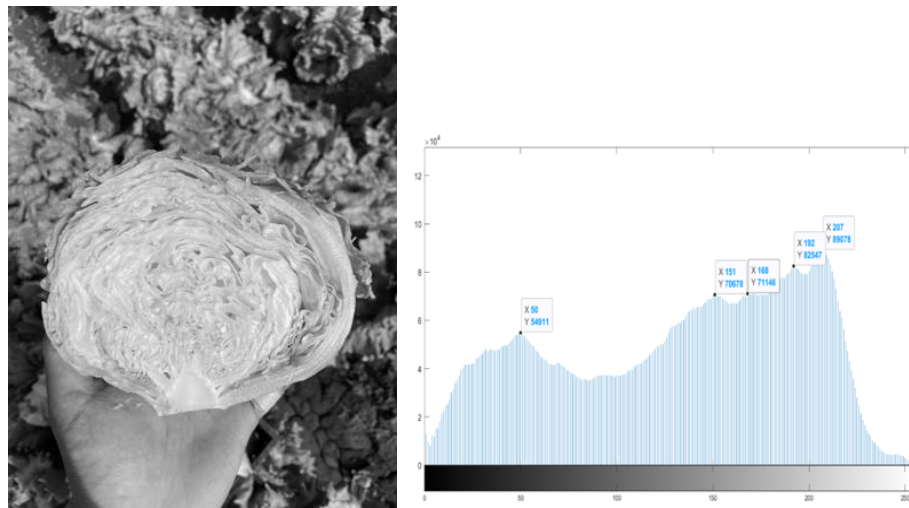


**Figure 1.10.** Histogram of a grayscale iceberg lettuce showing the distribution of gray level intensity (image by Xinzhen Chen and histogram created by MATLAB (MATLAB 2022a, The MathWorks, Inc., Natick, Massachusetts, United States)).

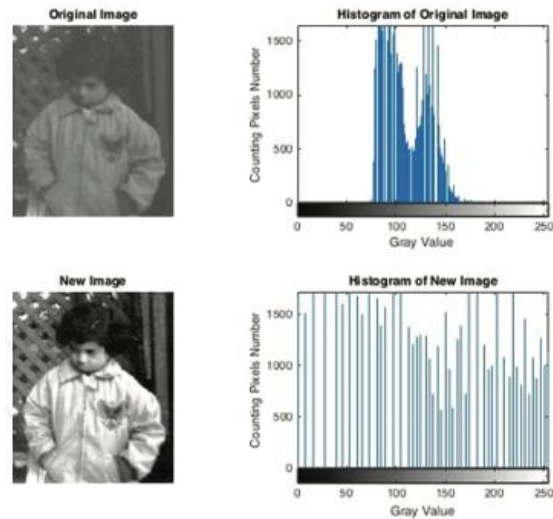


**Figure 1.11.** Histogram manipulation by equalizing gray level to increase the contrast of the object (figure source Sinecen 2016).

### *Segmentation*

Segmentation is the process of dividing a digital image into multiple homogenous regions by grouping pixels based on similarity in intensity, texture, or color. This divides an image into regions that can be more representative and easier to analyze. Such regions may correspond to individual surfaces, objects, or natural parts of objects (Khattab et al. 2014). Gorzelany et al. (2008) used binary image segmentation to detect defects such as bruises, frost damage, and scab on apple surface with average classification accuracy at 96% in the experiment. Mizushima and Lu (2013) developed an automatically adjustable algorithm that segmented color images using a linear support vector machine and Otsu's thresholding method for apple sorting and grading. Using color image segmentation, Burgos-Artizzu et al. (2009) developed an image analysis system that estimated the percentages of weeds, crop, and soil present in the image, and this allowed for the assessment of weed pressure for making herbicide treatment decisions.

Multiple disease detection and severity estimation were also done by color segmentation. Qin et al. (2016) used color segmentation and pattern recognition algorithms to identify different alfalfa leaf diseases, including common leaf spot (*Pseudopeziza medicaginis*), rust (*Uromyces striatus*), leptosphaerulina leaf spot (*Leptosphaerulina briosiana*), and cercospora leaf spot (*Cercospora medicaginis*). Combined with a support vector machine model, the recognition accuracies were high at 97.64%. Figure 1.12 shows an example on the natural senescence of Arabidopsis that was thresholded and segmented in MATLAB by calculating the pixel values and differentiating the proportion of yellow and green in a pie chart. This enabled the estimation of senescence levels.

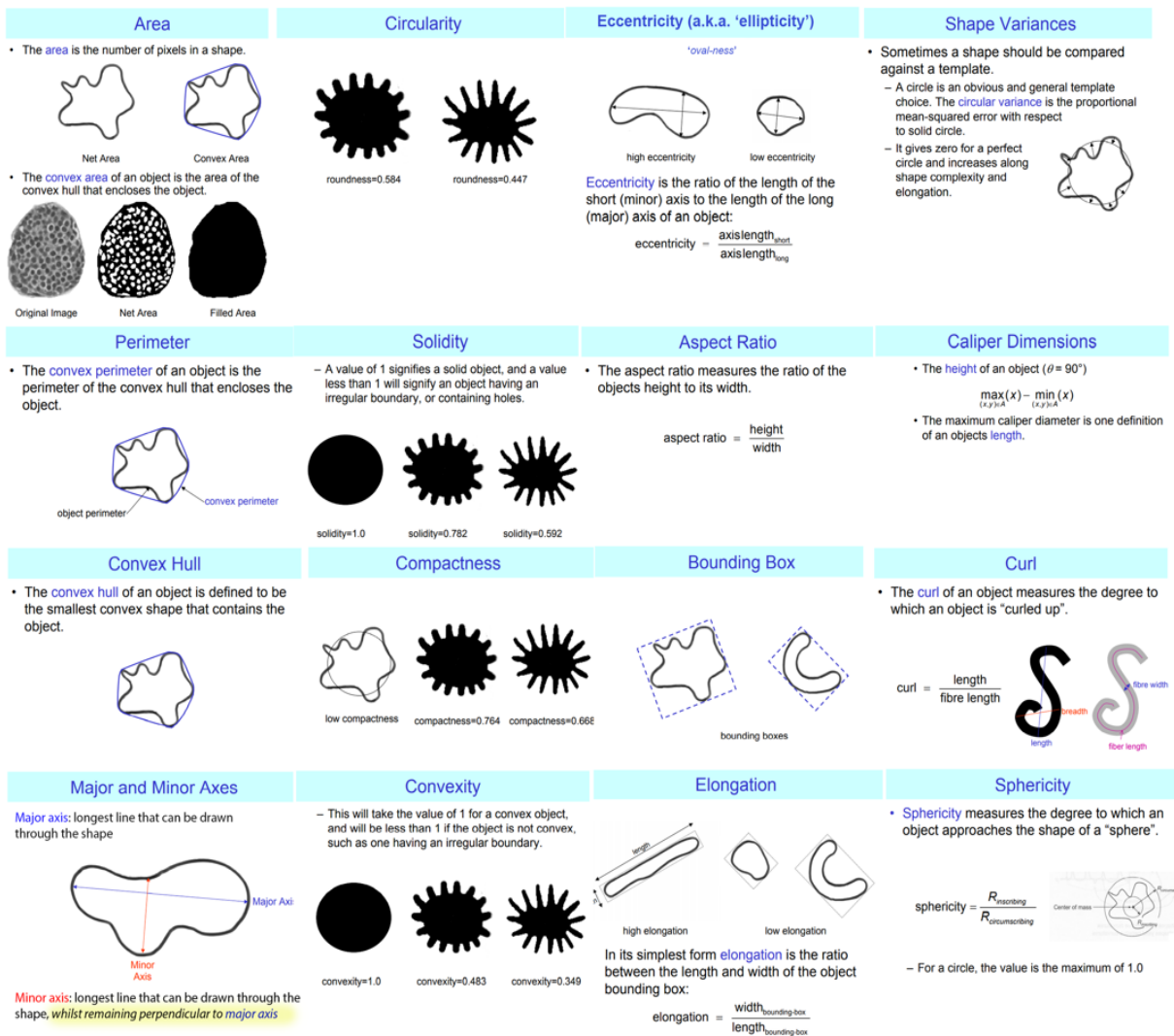


**Figure 1.12.** Color segmentation of natural senescence of Arabidopsis based on color green and yellow and pie chart showing the proportion of yellow and green pixels (figure credit Professor Sruti Das Choudhury and image processed by Xinzheng Chen).

### ***Feature Extraction***

Feature extraction is the process of defining a set of features in the image that can be efficiently analyzed and classified (Saxena and Armstrong 2014). These features can include shape, edge, texture, color, etc. (Khirade and Patil 2015). Weis et al. (2009) identified crops and weeds into species based on their shape. Plant shape varied between species allowing classification algorithms to distinguish them. However, the shape of a target can vary at different sizes or growth stages requiring extensive training to accurately distinguish them. Pérez et al. (2000) used color and shape features successfully to distinguish weeds from the crop with comparable results to human classification. This paper also showed the feasibility of conducting weed surveys in the field by using feature extraction to estimate the relative leaf area of weeds (i.e., weed leaf area/total leaf area of crop and weeds) while moving across the field. Wirth (2004) provided examples of using different features in shape analysis and measurement including length, width, area, edge roughness, circularity, and ellipticity (Figure 1.13). The leaf image features were used by a colleague at RD4AG, Connor Osgood, to separate different baby leaf lettuce varieties (Figure 1.14).

## Descriptive Shape Measurements for image analysis



Adapted from "Shape Analysis and Measurement" by Michael A. Wirth, Ph.D. (2004, University of Guelph)  
<http://www.cyto.purdue.edu/cdroms/micro2/content/education/wirth10.pdf>

**Figure 1.13.** Features commonly used in shape analysis and measurement (figure is adapted from "Shape Analysis and Measurement" by Michael A. Wirth 2004, University of Guelph).

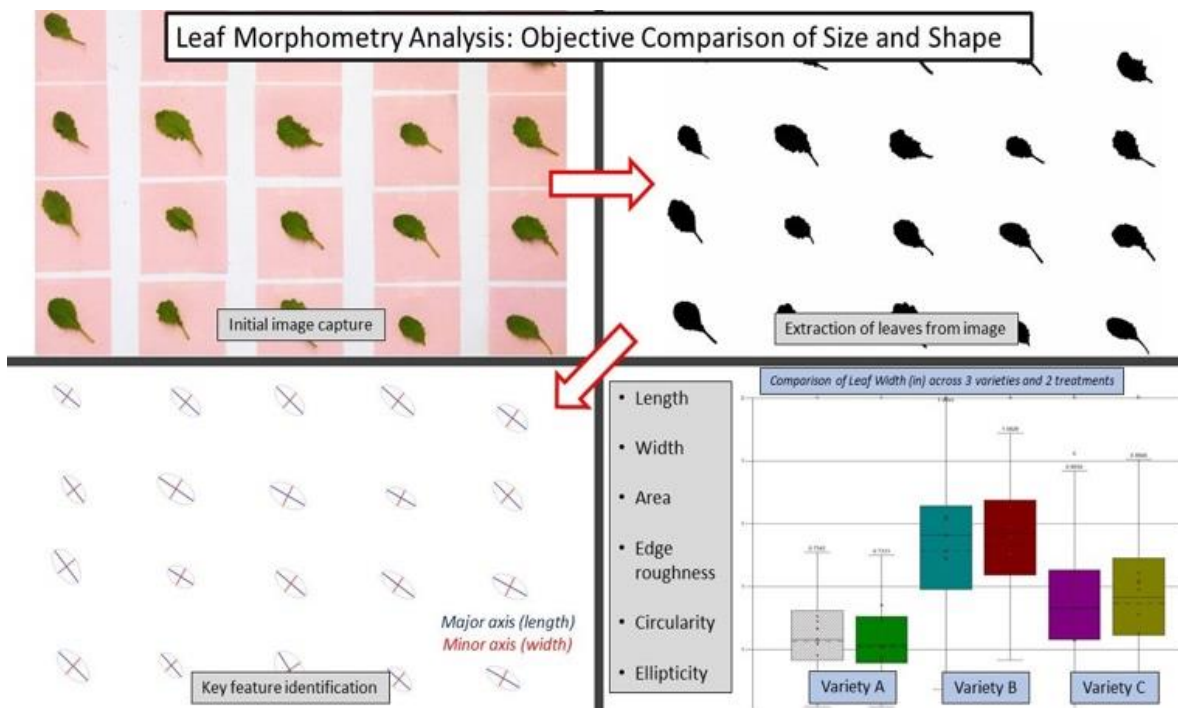


**Figure 1.14.** Using shape features in baby leaf lettuce to identify and separate each variety (figure credit Connor Osgood).

Edge detection is a useful tool to define the edge of an object. An edge is most often defined as an abrupt change in some image feature such as brightness or color (Martin et al. 2004). The most common approach for edge detection is to look for discontinuities in image brightness. This includes simple methods using the first or second derivative models, such as Sobel, Prewitt (Lipkin 1970), Laplacian of Gaussian, and Canny (Hou et al. 2022, Yu et al. 2021). More advanced learning-based methods (Dollár and Zitnick 2015, Hallman and Fowlkes 2015) can predict boundaries more precisely by utilizing various gradient information such as color, brightness, texture and depth (Dollár and Zitnick 2015, Martin et al. 2004, Ren and Bo 2012). Mustafa et al. (2008) used edge detection to determine banana size and, together with color, changes in banana quality.

Texture can be defined as a function of spatial variation of the brightness intensity of the pixels (Tuceryan and Jain 1993). The specific distribution pattern and the dispersion intensity of the pixels are used in image analysis to identify texture (Tuceryan and Jain 1993). The gray-level co-occurrence matrix is the algorithm frequently used by researchers to extract texture features in an image (Lurstwut and Pornpanomchai 2017). This algorithm considers the spatial distribution of the gray levels in the neighborhood and calculates texture feature values (Mousavirad et al. 2012). Texture features have been widely used in object recognition. Ehsani Rad and Kumar (2010) used a gray-level co-occurrence matrix to extract texture features from 390 leaves and classified them into 13 kinds of plants. Using texture and color features together with histogram matching allowed researchers to classify different tomato leaf diseases (Hlaing and Maung Zaw 2018). Texture measurement based on curvelet transformation were used to characterize fruit surface texture on lemon and guava to aid in evaluating skin damage (Khoje et al. 2013). Combined with support vector machine, a classification algorithm, an automatic fruit grading system was developed with 96% accuracy.

### **Image Analysis Software**

Image analysis software allows the user to read the image, extract digital information, and manipulate it mathematically if necessary (Shajahan 2019). In 2018, there were about 70 software packages for image processing (Wikipedia, 2018). Most of these were commercial packages that operated by the ‘click and run’ feature, but with limited features that were not suitable for processing batches of images or customizing the operations (Shajahan 2019).

MATLAB (The MathWorks, Inc., Natick, Massachusetts, United States) is a commercial software package that is user friendly for programming with great flexibility to customize and automate image analysis operations. However, MATLAB is usually used in academic institutions and specialized industry because of its high license cost (Shajahan 2019). ImageJ and PlantCV are two well-known open-source image processing software packages. ImageJ is Java-based and platform-independent with various toolbar and menu options, and it provides automatic running capabilities through macro and plugin coding (ImageJ, 2022). For macros developing to run batches, the scripting language is ImageJ Macro. PlantCV is an open-source, open-development suite of analysis tools capable of analyzing high-throughput image-based phenotyping data (Fahlgren et al. 2015). GitHub was used as a platform to organize the PlantCV community by integrating version control, code distribution, documentation, issue tracking, and communication between users and contributors (Perez-Riverol et al. 2016). PlantCV uses Python which is a high-level language widely used for both teaching and bioinformatics (Dudley and Butte 2009, Mangalam 2002).

### **Image Analysis and Machine Learning**

ImageJ is a user-friendly software allowing quick and simple image analysis such as color segmentation, edge detection, and shape analysis. However, more complex evaluation including measuring more than one parameter requires machine learning.

After image analysis is used to extract useful data from an image, the data can be fed into machine learning algorithms for classification. Machine learning is based on computational statistics and analysis used to develop algorithms to learn and make

predictions from image data (Kersting et al. 2016). A flow diagram of the machine learning process is shown in Figure 1.15 (Liakos et al. 2018).

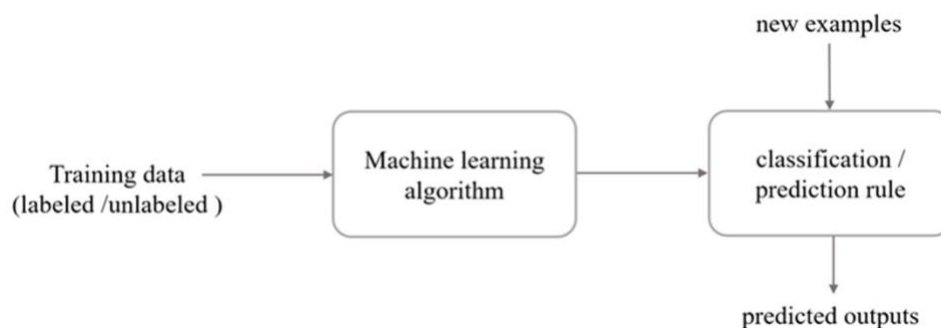


**Figure 1.15.** General machine learning progress (figure source Liakos et al. 2018).

Machine learning in general can be divided into two categories: supervised learning, and unsupervised learning. Supervised machine learning uses labeled datasets. The labeled datasets, for example, can be a set of disease images that have been graded previously by professionals. These labeled datasets will then be used to “supervise” algorithms to classify data or make accurate predictions (Mahesh 2019). The most common supervised machine learning algorithms include decision tree, naïve bayes, and support vector machine (Ray 2019, Rehman et al. 2019). Decision tree was used by Yang et al. (2003) to distinguish different tillage methods and residual levels with accuracy of 89% and 98% respectively using hyperspectral imaging. Granitto et al. (2002) used naïve bayes to classify 57 different species of weed seeds and the test data had the accuracy of 99.2%. Support vector machine was used by Ebrahimi et al. (2017) to classify pests of strawberry and automatic detection of thrips with the accuracy of 97.75%.

Unsupervised learning does not have previously labeled datasets and uses methods of clustering (k-means clustering) that rely on structural patterns in the data. K

clustering can cluster pixels into groups of similar pixels. K refers to the number of groups in an image. K-mean clustering was used by Zhang et al. (2017) on cucumber leaf images. Based on the disease pixel segmentation and classification, the disease detection had overall accuracy of 85.7%. Study by Liming and Yanchao (2010) used k-mean clustering to extract strawberry fruit characteristics (i.e., shape, size, and color) and were able to sort them into different grades with the overall accuracy of 91%.

### **Challenges of Image Analysis**

Image analysis has great potential to enhance the collection of useful data with high efficiency. However, there are many challenges when dealing with plants growing in the field.

Extrinsic factors include complex backgrounds and lighting conditions. Complex background can make segmentation difficult. This is particularly challenging when taking plant images with significant green elements in the background or with the presence of other plants, leaves, and soil (Barbedo 2016). Ideally, all images should be captured under the same lighting conditions. However, images taken in the field will deal with various lighting conditions that are affected by time of day, position of the sun with respect to the leaf, and overcast conditions.

Intrinsic factors are more complex. Take plant disease as an example, some symptoms might not have well defined boundaries that blend with healthy tissue making it hard to separate. Diseases at different stages can have very different characteristics. Diseases, stressors, or toxicities might share similar symptoms that are not easy to differentiate. In addition, plants infested by multiple diseases can create “hybrid” symptoms. Other limiting factors for adoption of image analysis in agriculture includes

high cost of the equipment (e.g., hyperspectral cameras, drones, and controlled lighting apparatus). The complexity of data analytics software and the amount of data that is generated requires extensive computing power and data storage capabilities (Omari et al. 2020).

### **Summary**

Image analysis has tremendous application potential in agriculture research. The electromagnetic spectrum contains different electromagnetic radiation that categorizes images into RGB, spectral, and thermal images. Each kind of imaging has advantages that make it suitable for different applications in agricultural research. Digital images include information of an object and selecting the proper color model can help better visualize the information numerically. When taking an image in the field, image quality can be improved by controlling the background, lighting conditions, and object features. Image analysis includes image processing, segmentation, and feature extraction. Two important image processing methods, histogram manipulation and brightness alteration, help improve the contrast of an object from its background. Segmentation is the process of dividing an image into regions that are representative and easier for analysis. Feature extraction further defines those regions based on shape, edge, texture, and color to provide more information on the image feature (e.g., disease, deficiency, stress, etc.). Combined with machine learning, information can be used for disease detection, classifying plant species, and grading fruit among other applications. Image analysis provides many advantages in agricultural research, however, there are challenges in image analysis. The challenges include complex background and lighting conditions in the field, disease symptoms that are not well defined, and the high cost of the equipment.

With the improvement of cameras, image analysis software, and machine learning algorithms, image analysis will keep improving and make agricultural research more efficient. Chapter 2 will provide case studies using image analysis in applied agricultural research.

## References

- Ahmed A, Ibrahim A, Hussein S (2019) Detection of Palm Tree Pests Using Thermal Imaging: A Review. Pages 253–270 *in* AE Hassanien, ed. *Machine Learning Paradigms: Theory and Application*. Cham: Springer International Publishing
- Ashourloo D, Mobasher MR, Huete A (2014) Developing Two Spectral Disease Indices for Detection of Wheat Leaf Rust (*Puccinia triticina*). *Remote Sens* 6:4723–4740
- Asmare MH, Asirvadam VS, Iznita L (2009) Color Space Selection for Color Image Enhancement Applications. Pages 208–212 *in* 2009 International Conference on Signal Acquisition and Processing
- Awcock GJ, Thomas R (1995) Image Acquisition. Pages 59–89 *in* GJ Awcock, R Thomas, eds. *Applied Image Processing*. London: Macmillan Education UK
- Balter S (1993) Fundamental properties of digital images. *Radiogr Rev Publ Radiol Soc N Am Inc* 13:129–141
- Barbedo JGA (2016) A review on the main challenges in automatic plant disease identification based on visible range images. *Biosyst Eng* 144:52–60
- Bock CH, Barbedo JGA, Del Ponte EM, Bohnenkamp D, Mahlein A-K (2020) From visual estimates to fully automated sensor-based measurements of plant disease severity: status and challenges for improving accuracy. *Phytopathol Res* 2:9
- Bock CH, Parker PE, Cook AZ, Riley T, Gottwald TR (2009) Comparison of Assessment of Citrus Canker Foliar Symptoms by Experienced and Inexperienced Raters. *Plant Dis* 93:412–424
- Bock CH, Poole GH, Parker PE, Gottwald TR (2010) Plant Disease Severity Estimated Visually, by Digital Photography and Image Analysis, and by Hyperspectral Imaging. *Crit Rev Plant Sci* 29:59–107
- Bunster L, Fokkema NJ, Schippers B (1989) Effect of Surface-Active *Pseudomonas* spp. on Leaf Wettability. *Appl Environ Microbiol* 55:1340–1345
- Burgos-Artizzu XP, Ribeiro A, Tellaeche A, Pajares G, Fernández-Quintanilla C (2009) Improving weed pressure assessment using digital images from an experience-based reasoning approach. *Comput Electron Agric* 65:176–185
- Category: Image processing software (2018)  
[https://en.wikipedia.org/wiki/Category:Image\\_processing\\_software](https://en.wikipedia.org/wiki/Category:Image_processing_software)
- Chaerle L, Caeneghem WV, Messens E, Lambers H, Van Montagu M, Van Der Straeten D (1999) Presymptomatic visualization of plant–virus interactions by thermography. *Nat Biotechnol* 17:813–816

- Chaerle L, De Boever F, Montagu MV, Straeten DVD (2001) Thermographic visualization of cell death in tobacco and Arabidopsis. *Plant Cell Environ* 24:15–25
- Chaerle L, Hagenbeek D, De Bruyne E, Valcke R, Van Der Straeten D (2004) Thermal and Chlorophyll-Fluorescence Imaging Distinguish Plant-Pathogen Interactions at an Early Stage. *Plant Cell Physiol* 45:887–896
- Chung C-L, Huang K-J, Chen S-Y, Lai M-H, Chen Y-C, Kuo Y-F (2016) Detecting Bakanae disease in rice seedlings by machine vision. *Comput Electron Agric* 121:404–411
- Cline WR (2008) Global Warming and Agriculture. *Finance Dev* 45. *Finance & Development*, 45(001)
- Cohen Y, Alchanatis V, Prigojin A, Levi A, Soroker V, Cohen Y (2012) Use of aerial thermal imaging to estimate water status of palm trees. *Precis Agric* 13:123–140
- Dollár P, Zitnick CL (2015) Fast Edge Detection Using Structured Forests. *IEEE Trans Pattern Anal Mach Intell* 37:1558–1570
- Dudley JT, Butte AJ (2009) A Quick Guide for Developing Effective Bioinformatics Programming Skills. *PLOS Comput Biol* 5:e1000589
- Dwairi M, Alqadi Z, Abujazar A, Abu Zneit R (2010) Optimized True-Color Image Processing. *World Applied Sciences Journal* 8 (10): 1175-1182, 2010
- Ebrahimi MA, Khoshtaghaza MH, Minaei S, Jamshidi B (2017) Vision-based pest detection based on SVM classification method. *Comput Electron Agric* 137:52–58
- Ehsani Rad A, Kumar YH (2010) Leaf recognition for plant classification using GLCM and PCA methods. *Orient J Comput Sci Technol* 3:6
- Elsayed S, Elhoweity M, Ibrahim HH, Dewir YH, Migdadi HM, Schmidhalter U (2017) Thermal imaging and passive reflectance sensing to estimate the water status and grain yield of wheat under different irrigation regimes. *Agric Water Manag* 189:98–110
- Evening M (2007) *Adobe Photoshop CS3 for Photographers: A Professional Image Editor's Guide to the Creative Use of Photoshop for the Macintosh and PC*. Taylor & Francis. 706 p
- Fahlgren N, Feldman M, Gehan MA, Wilson MS, Shyu C, Bryant DW, Hill ST, McEntee CJ, Warnasooriya SN, Kumar I, Ficor T, Turnipseed S, Gilbert KB, Brutnell TP, Carrington JC, Mockler TC, Baxter I (2015) A Versatile Phenotyping System and Analytics Platform Reveals Diverse Temporal Responses to Water Availability in *Setaria*. *Mol Plant* 8:1520–1535

- Fernández CI, Leblon B, Haddadi A, Wang K, Wang J (2020) Potato Late Blight Detection at the Leaf and Canopy Levels Based in the Red and Red-Edge Spectral Regions. *Remote Sens* 12:1292
- Gamon JA, Peñuelas J, Field CB (1992) A narrow-waveband spectral index that tracks diurnal changes in photosynthetic efficiency. *Remote Sens Environ* 41:35–44
- Gao D, Li M, Zhang J, Song D, Sun H, Qiao L, Zhao R (2021) Improvement of chlorophyll content estimation on maize leaf by vein removal in hyperspectral image. *Comput Electron Agric* 184:106077
- Garini Y, Young IT, McNamara G (2006) Spectral imaging: Principles and applications. *Cytometry A* 69A:735–747
- Giannoni L, Lange F, Tachtsidis I (2018) Hyperspectral imaging solutions for brain tissue metabolic and hemodynamic monitoring: past, current and future developments. *J Opt* 20:044009
- Goetz AFH (2009) Three decades of hyperspectral remote sensing of the Earth: A personal view. *Remote Sens Environ* 113:S5–S16
- Golomb O, Alchanatis V, Cohen Y, Levin N, Cohen Y, Soroker V (2015) Detection of red palm weevil infected trees using thermal imaging. Pages 643–650 *in* Precision agriculture '15. Wageningen Academic Publishers
- Gómez-López VM, Bhat R (2021) *Electromagnetic Technologies in Food Science*. John Wiley & Sons. 469 p
- Gorzelany J, Zaguła G, Brusewitz G (2008) Image analysis for apple defect detection *Biosystems and agricultura engineering* 8 (2008): 197-205.
- Gowen AA, O'Donnell CP, Cullen PJ, Downey G, Frias JM (2007) Hyperspectral imaging – an emerging process analytical tool for food quality and safety control. *Trends Food Sci Technol* 18:590–598
- Grande JC (2012) Principles of Image Analysis. *Metallogr Microstruct Anal* 1:227–243
- Granitto PM, Navone HD, Verdes PF, Ceccatto HA (2002) Weed seeds identification by machine vision. *Comput Electron Agric* 33:91–103
- Gudesblat GE, Torres PS, Vojnov AA (2009) *Xanthomonas campestris* Overcomes Arabidopsis Stomatal Innate Immunity through a DSF Cell-to-Cell Signal-Regulated Virulence Factor. *Plant Physiol* 149:1017–1027
- Gupta M, Abdelsalam M, Khorsandroo S, Mittal S (2020) Security and Privacy in Smart Farming: Challenges and Opportunities. *IEEE Access* 8:34564–34584

- Hallman S, Fowlkes CC (2015) Oriented Edge Forests for Boundary Detection. Pages 1732–1740 in IEEE Conference on Computer Vision and Pattern Recognition
- Herter CA Jr (1985) The Electromagnetic Spectrum: A Critical Natural Resource. *Nat Resour J* 25:651–664
- Hlaing CS, Maung Zaw SM (2018) Tomato Plant Diseases Classification Using Statistical Texture Feature and Color Feature. Pages 439–444 in 2018 IEEE/ACIS 17th International Conference on Computer and Information Science (ICIS)
- Hou J, Guo Z, Wu Y, Diao W, Xu T (2022) BSNet: Dynamic Hybrid Gradient Convolution Based Boundary-Sensitive Network for Remote Sensing Image Segmentation. *IEEE Trans Geosci Remote Sens* 60:1–22
- Hung D-Z, Yang H-J, Li Y-F, Lin C-L, Chang S-Y, Sung F-C, Tai SCW (2015) The Long-Term Effects of Organophosphates Poisoning as a Risk Factor of CVDs: A Nationwide Population-Based Cohort Study. *PLOS ONE* 10:e0137632
- Ibraheem NA, Hasan MM, Khan RZ, Mishra PK (2012) Understanding Color Models: A Review. *ARPN J Sci Technol*:265–275
- Idso SB, Jackson RD, Pinter PJ, Reginato RJ, Hatfield JL (1981) Normalizing the stress-degree-day parameter for environmental variability. *Agric Meteorol* 24:45–55
- ImageJ ( n.d.) . <https://imagej.nih.gov/ij/>. Accessed October 21, 2022
- Ishimwe R, Abutaleb K, Ahmed F (2014) Applications of Thermal Imaging in Agriculture—A Review. *Adv Remote Sens* 03:128
- Ji-Yong S, Xiao-Bo Z, Jie-Wen Z, Kai-Liang W, Zheng-Wei C, Xiao-Wei H, De-Tao Z, Holmes M (2012) Nondestructive diagnostics of nitrogen deficiency by cucumber leaf chlorophyll distribution map based on near infrared hyperspectral imaging. *Sci Hort* 138:190–197
- Kacira M, Sase S, Limi O, Ling P (2005) Plant Response-Based Sensing for Control Strategies in Sustainable Greenhouse Production. *J Agric Meteorol* 61:15–22
- Kalantari F, Tahir OM, Joni RA, Fatemi E (2017) Opportunities and Challenges in Sustainability of Vertical Farming: A Review. *J Landsc Ecol* 11:35–60
- Kant Y, Bharath BD, Mallick J, Atzberger C, Kerle N (2009) Satellite-based analysis of the role of land use/land cover and vegetation density on surface temperature regime of Delhi, India. *J Indian Soc Remote Sens* 37:201–214
- Kersting K, Bauckhage C, Wahabzada M, Mahlein A-K, Steiner U, Oerke E-C, Römer C, Plümer L (2016) Feeding the World with Big Data: Uncovering Spectral Characteristics and Dynamics of Stressed Plants. Pages 99–120 in J Lässig, K

Kersting, K Morik, eds. Computational Sustainability. Cham: Springer International Publishing

- Khattab D, Ebied H, Hussein A, Tolba M (2014) Color Image Segmentation Based on Different Color Space Models Using Automatic GrabCut. *ScientificWorldJournal* 2014:126025
- Khirade SD, Patil AB (2015) Plant Disease Detection Using Image Processing. Pages 768–771 in 2015 International Conference on Computing Communication Control and Automation
- Khoje S, Bodhe S, Adsul A (2013) Automated Skin Defect Identification System for Fruit Grading Based on Discrete Curvelet Transform. *Int J Eng Technol* 5:3251–3256
- Kim DM, Zhang H, Zhou H, Du T, Wu Q, Mockler TC, Berezin MY (2015) Highly sensitive image-derived indices of water-stressed plants using hyperspectral imaging in SWIR and histogram analysis. *Sci Rep* 5:15919
- Kim Y, Glenn DM, Park J, Ngugi HK, Lehman BL (2011) Hyperspectral image analysis for water stress detection of apple trees. *Comput Electron Agric* 77:155–160
- Klukas C, Chen D, Pape J-M (2014) Integrated Analysis Platform: An Open-Source Information System for High-Throughput Plant Phenotyping. *Plant Physiol* 165
- Koch H, Hau B (1980) Ein psychologischer Aspekt beim Schätzen von Pflanzenkrankheiten / A psychological aspect of plant disease assessment. *Z Für Pflanzenkrankh Pflanzenschutz J Plant Dis Prot* 87:587–593
- Kour H (2015) Analysis on Image Color Model 4:233–235 *International Journal of Advanced Research in Computer and Communication Engineering* Vol. 4, Issue 12
- Kovacs M, Hoekstra R, Aczel B (2021) The Role of Human Fallibility in Psychological Research: A Survey of Mistakes in Data Management. *Adv Methods Pract Psychol Sci* 4:25152459211045930
- Łabędź P, Skabek K, Ozimek P, Nytko M (2021) Histogram Adjustment of Images for Improving Photogrammetric Reconstruction. *Sensors* 21:4654
- Liakos KG, Busato P, Moshou D, Pearson S, Bochtis D (2018) Machine Learning in Agriculture: A Review. *Sensors* 18:2674
- Liming X, Yanchao Z (2010) Automated strawberry grading system based on image processing. *Comput Electron Agric* 71:S32–S39

- Lindenthal M, Steiner U, Dehne H-W, Oerke E-C (2005) Effect of Downy Mildew Development on Transpiration of Cucumber Leaves Visualized by Digital Infrared Thermography. *Phytopathology*® 95:233–240
- Lipkin BS (1970) *Picture Processing and Psychopictorics*. Elsevier. 535 p
- Long W, zhang Q, Wang S-R, Suo Y, Chen H, Bai X, Yang X, Zhou Y-P, Yang J, Fu H (2023) Fast and non-destructive discriminating the geographical origin of Hangbaiju by hyperspectral imaging combined with chemometrics. *Spectrochim Acta A Mol Biomol Spectrosc* 284:121786
- Lowe A, Harrison N, French AP (2017) Hyperspectral image analysis techniques for the detection and classification of the early onset of plant disease and stress. *Plant Methods* 13:80
- Lu B, Dao PD, Liu J, He Y, Shang J (2020) Recent Advances of Hyperspectral Imaging Technology and Applications in Agriculture. *Remote Sens* 12:2659
- Lurstwut B, Pornpanomchai C (2017) Image analysis based on color, shape and texture for rice seed (*Oryza sativa* L.) germination evaluation. *Agric Nat Resour* 51:383–389
- Mahesh B (2019) Machine Learning Algorithms -A Review *International Journal of Science and Research (IJSR)* ISSN: 2319-7064
- Mancosu N, Snyder RL, Kyriakakis G, Spano D (2015) Water Scarcity and Future Challenges for Food Production. *Water* 7:975–992
- Mangalam H (2002) The Bio\* toolkits — a brief overview. *Brief Bioinform* 3:296–302
- Manickavasagan A, Jayasuriya H, eds. (2014) *Imaging with Electromagnetic Spectrum*. Berlin, Heidelberg: Springer
- Martin DR, Fowlkes CC, Malik J (2004) Learning to detect natural image boundaries using local brightness, color, and texture cues. *IEEE Trans Pattern Anal Mach Intell* 26:530–549
- Mete M, Topaloglu U (2009) Statistical comparison of color model-classifier pairs in hematoxylin and eosin stained histological images. Pages 284–291 in 2009 IEEE Symposium on Computational Intelligence in Bioinformatics and Computational Biology
- Miranda-Contreras L, Gómez-Pérez R, Rojas G, Cruz I, Berrueta L, Salmen S, Colmenares M, Barreto S, Balza A, Zavala L, Morales Y, Molina Y, Valeri L, Contreras CA, Osuna JA (2013) Occupational Exposure to Organophosphate and Carbamate Pesticides Affects Sperm Chromatin Integrity and Reproductive Hormone Levels among Venezuelan Farm Workers. *J Occup Health* 55:195–203

- Mishra V, Kumar S, Shukla N (2017) Image Acquisition and Techniques to Perform Image Acquisition. SAMRIDDHI J Phys Sci Eng Technol 9
- Mizushima A, Lu R (2013) An image segmentation method for apple sorting and grading using support vector machine and Otsu's method. Comput Electron Agric 94:29–37
- Moghadam P, Ward D, Goan E, Jayawardena S, Sikka P, Hernandez E (2017) Plant Disease Detection Using Hyperspectral Imaging. Pages 1–8 *in* 2017 International Conference on Digital Image Computing: Techniques and Applications (DICTA)
- Molecular Expressions Microscopy Primer: Digital Imaging in Optical Microscopy - Basic Properties of Digital Images ( n.d.) .  
<https://micro.magnet.fsu.edu/primer/digitalimaging/digitalimagebasics.html>.  
Accessed September 15, 2022
- Morkel T, Eloff J, Olivier M (2005) An overview of image steganography. Pages 1–11 *in*
- Mousavirad SJ, Akhlaghian Tab F, Mollazade K (2012) Application of Imperialist Competitive Algorithm for Feature Selection: A Case Study on Bulk Rice Classification. Int J Comput Appl 40:41–48
- Mustafa NBA, Fuad NA, Ahmed SK, Abidin AAZ, Ali Z, Yit WB, Sharrif ZAM (2008) Image processing of an agriculture produce: Determination of size and ripeness of a banana. Pages 1–7 *in* 2008 International Symposium on Information Technology
- Mutka AM, Bart RS (2015) Image-based phenotyping of plant disease symptoms. Front Plant Sci 5
- Naik HS, Zhang J, Lofquist A, Assefa T, Sarkar S, Ackerman D, Singh A, Singh AK, Ganapathysubramanian B (2017) A real-time phenotyping framework using machine learning for plant stress severity rating in soybean. Plant Methods 13:23
- Olson MB, Crawford MM, Vyn TJ (2022) Hyperspectral Indices for Predicting Nitrogen Use Efficiency in Maize Hybrids. Remote Sens 14:1721
- Omari MK, Lee J, Faqeerzada MA, Joshi R, Park E, Cho B-K (2020) Digital image-based plant phenotyping: a review. Korean J Agric Sci 47:119–130
- Peiris KHS, Pumphrey MO, Dowell FE (2009) NIR Absorbance Characteristics of Deoxynivalenol and of Sound and Fusarium-Damaged Wheat Kernels. J Infrared Spectrosc 17:213–221
- Pérez AJ, López F, Benlloch JV, Christensen S (2000) Colour and shape analysis techniques for weed detection in cereal fields. Comput Electron Agric 25:197–212

- Perez-Riverol Y, Gatto L, Wang R, Sachsenberg T, Uszkoreit J, Leprevost F da V, Fufezan C, Ternent T, Eglen SJ, Katz DS, Pollard TJ, Kononov A, Flight RM, Blin K, Vizcaíno JA (2016) Ten Simple Rules for Taking Advantage of Git and GitHub. *PLOS Comput Biol* 12:e1004947
- Pradawet C, Khongdee N, Pansak W, Spreer W, Hilger T, Cadisch G ( n.d.) Thermal imaging for assessment of maize water stress and yield prediction under drought conditions. *J Agron Crop Sci* n/a
- Pradhan S, Bandyopadhyay KK, Sahoo RN, Sehgal VK, Singh R, Gupta VK, Joshi DK (2014) Predicting Wheat Grain and Biomass Yield Using Canopy Reflectance of Booting Stage. *J Indian Soc Remote Sens* 42:711–718
- Qin F, Liu D, Sun B, Ruan L, Ma Z, Wang H (2016) Identification of Alfalfa Leaf Diseases Using Image Recognition Technology. *PLOS ONE* 11:e0168274
- Ray S (2019) A Quick Review of Machine Learning Algorithms. Pages 35–39 *in* 2019 International Conference on Machine Learning, Big Data, Cloud and Parallel Computing (COMITCon)
- Rehman TU, Mahmud MdS, Chang YK, Jin J, Shin J (2019) Current and future applications of statistical machine learning algorithms for agricultural machine vision systems. *Comput Electron Agric* 156:585–605
- Ren X, Bo L (2012) Discriminatively trained sparse code gradients for contour detection. Pages 584–592 *in* Proceedings of the 25th International Conference on Neural Information Processing Systems - Volume 1. Red Hook, NY, USA: Curran Associates Inc.
- Roopaei M, Rad P, Choo K-KR (2017) Cloud of Things in Smart Agriculture: Intelligent Irrigation Monitoring by Thermal Imaging. *IEEE Cloud Comput* 4:10–15
- Rosenstock L, Keifer M, Daniell WE, McConnell R, Claypoole K (1991) Chronic central nervous system effects of acute organophosphate pesticide intoxication. *The Lancet* 338:223–227
- Sahoo RN, Ray SS, Manjunath KR (2015) Hyperspectral remote sensing of agriculture. *Curr Sci* 108:848–859
- Sankaran S, Maja JM, Buchanon S, Ehsani R (2013) Huanglongbing (Citrus Greening) Detection Using Visible, Near Infrared and Thermal Imaging Techniques. *Sensors* 13:2117–2130
- Saxena L, Armstrong L (2014) A survey of image processing techniques for agriculture. *Res Outputs* 2014 2021

- Shahin MA, Symons SJ (2011) Detection of Fusarium damaged kernels in Canada Western Red Spring wheat using visible/near-infrared hyperspectral imaging and principal component analysis. *Comput Electron Agric*
- Shajahan S (2019) Agricultural Field Applications of Digital Image Processing Using an Open Source ImageJ Platform
- Shamshiri R (2009) Application of GPS data for farm and machinery management. University of Florida IFAS Extension
- Sims DA, Gamon JA (2002) Relationships between leaf pigment content and spectral reflectance across a wide range of species, leaf structures and developmental stages. *Remote Sens Environ* 81:337–354
- Sinecen M (2016) Digital Image Processing with MATLAB, Applications from Engineering with MATLAB Concepts. IntechOpen. <https://doi.org/10.5772/63028>
- Sonka M, Hlavac V, Boyle R (2014) Image Processing, Analysis, and Machine Vision. Cengage Learning. 930 p
- Suganya E, Sountharajan S, Shandilya SK, Karthiga M (2019) Chapter 5 - IoT in Agriculture Investigation on Plant Diseases and Nutrient Level Using Image Analysis Techniques. Pages 117–130 *in* VE Balas, LH Son, S Jha, M Khari, R Kumar, eds. Internet of Things in Biomedical Engineering. Academic Press
- Tuceryan M, Jain AK (1993) Texture analysis. Pages 235–276 *in* Handbook of Pattern Recognition and Computer Vision. WORLD SCIENTIFIC
- Vithu P, Moses JA (2016) Machine vision system for food grain quality evaluation: A review. *Trends Food Sci Technol* 56:13–20
- Wang F-M, Huang J-F, Wang X-Z (2008) Identification of Optimal Hyperspectral Bands for Estimation of Rice Biophysical Parameters. *J Integr Plant Biol* 50:291–299
- Wang Y, Hu X, Jin G, Hou Z, Ning J, Zhang Z (2019) Rapid prediction of chlorophylls and carotenoids content in tea leaves under different levels of nitrogen application based on hyperspectral imaging. *J Sci Food Agric* 99:1997–2004
- Weis M, Rumpf T, Gerhards R, Plümer L ( n.d.) Comparison of different classification algorithms for weed detection from images based on shape parameters:12
- Wesseling C, Keifer M, Ahlbom A, McConnell R, Moon J-D, Rosenstock L, Hogstedt C (2002) Long-term Neurobehavioral Effects of Mild Poisonings with Organophosphate and n-Methyl Carbamate Pesticides among Banana Workers. *Int J Occup Environ Health* 8:27–34
- Wieme J, Mollazade K, Malounas I, Zude-Sasse M, Zhao M, Gowen A, Argyropoulos D, Fountas S, Van Beek J (2022) Application of hyperspectral imaging systems and

artificial intelligence for quality assessment of fruit, vegetables and mushrooms:  
A review. *Biosyst Eng* 222:156–176

Wiggins R, Davidson H, Harnsberger H, Lauman J, Goede P (2000) Image File Formats:  
Past, Present, and Future1. *Radiogr Rev Publ Radiol Soc N Am Inc* 21:789–98

Yam KL, Papadakis SE (2004) A simple digital imaging method for measuring and  
analyzing color of food surfaces. *J Food Eng* 61:137–142

Yang C-C, Prasher SO, Enright P, Madramootoo C, Burgess M, Goel PK, Callum I  
(2003) Application of decision tree technology for image classification using  
remote sensing data. *Agric Syst* 76:1101–1117

Yu X, Wang Z, Wang Y, Zhang C (2021) Edge Detection of Agricultural Products Based  
on Morphologically Improved Canny Algorithm. *Math Probl Eng* 2021:e6664970

Zhang S, Wu X, You Z, Zhang L (2017) Leaf image based cucumber disease recognition  
using sparse representation classification. *Comput Electron Agric* 134:135–141

## **Chapter 2: Applications using image analysis in applied agricultural research**

### **Introduction**

Digital image analysis has gained in popularity in the past few years especially with advances in cameras, computing power, and analysis methods (Dougherty 2009, Zhao et al. 2016). The application of digital image analysis has been widely used in the medical field to diagnose cancer (Jain and Patil 2014), tumors (Bauer et al. 2013), and cardiovascular disease (Heiberg et al. 2010). However, application in agriculture is not as extensively explored. At present, agricultural research mostly requires highly trained researchers to go to the field, collect data, and make evaluations, such as the impacts of nutrient deficiency, water and salt stress, and pest and disease infestation (Camargo and Smith 2009). These evaluations need to be done in a timely manner for early detection and to make management decisions for efficient crop production (Shajahan 2019). Historically, evaluations have been done by visual observation and follow protocols that are subjective, tedious, time-consuming, and require manual data entry (Shajahan 2019). During the process, errors cannot be avoided, and this could alter the research results or even future research direction. Image analysis could be one solution to mitigate these issues as the approach is objective, quick, reproduceable, and easy to apply (Shajahan 2019).

In this chapter, application of image analysis for different agriculture research will be explored. Leaf damage is the most common symptom observed on an unhealthy plant. Symptoms could be caused by disease (Jermini et al. 2010), pest (Xu et al. 2007), nutrient deficiency (Jeyalakshmi and Radha 2017) or toxicity (Sotiropoulos et al. 2002), and even certain herbicide injuries (Chen 2021). All these are important in crop production,

breeding for resistance, or testing for chemical efficacy. Stress detection is important for crop production, and yield goals can be hindered by water stress (Skirycz and Inzé 2010), salinity stress (Läuchli and Grattan 2007), and even heavy metal toxicity (Hagemeyer 2004). In addition, global warming, climate change, and industrial pollution could intensify current plant stress due to its impact on plants, soils, and microbial communities (Zandalinas et al. 2021). Thus, stress detection and quantification will be an area explored using image analysis.

Monitoring plant growth is the foundation for any farming system to ensure crop productivity with minimum input (such as fertilizer and water) and harvesting in a timely manner for optimum quality (Li et al. 2020). Parameters such as leaf area, shoot dry weight, and relative growth rate are commonly used in research to characterize plant growth in response to different environmental changes (Li et al. 2020). Measuring leaf area can be useful in making decisions in optimizing supplemental light in indoor production (Barbosa et al. 2015, Shimizu et al. 2011) based on the light interception by the leaves. Estimating shoot dry weight can help to maximize economic return as it is closely related to fresh biomass (Chaimala et al. 2020). Relative growth rate is useful for comparing different plant cultivars for selecting better genotypes (Boyer 1982). Often, these parameters are ignored in the commercial system because they are hard to measure based only on visual assessments and the requirement for destructive sampling (Li et al. 2020). Therefore, using a non-destructive tool for measuring plant growth characteristics is important. Image analysis is one solution due to its high sensitivity to identify small growth differences in plants (Li et al. 2020).

Plant stand counts are crucial for farmers to evaluate seed germination rate and the plant uniformity (Shirzadifar et al. 2020). Early detection of poor stands in the field can help farmers make decisions on replanting or taking other actions on the defective zones (Shirzadifar et al. 2020). Traditional methods for manual stand counts are time consuming, labor intensive, and error-prone (Pathak et al. 2022). To solve the problem, high spatial resolution images taken by unmanned aerial vehicles (UAV) can be used by combining image analysis and computer vision algorithms to evaluate plant stand count (Pathak et al. 2022).

Pest counting is another area important in the integrated pest management (IPM) paradigm to decide economic injury levels and economic thresholds. For example, soybean aphids (*Aphis glycines*) is a serious pest that causes enormous soybean yield loss in the U.S. (Shajahan et al. 2017). Soybean farmers are advised to apply insecticide when populations exceed an economic threshold of 250 aphids per plant (Hodgson et al. 2012, Johnson et al. 2009). To quantify aphids numbers, traditionally, counting is done manually by trained experts through visual inspection (Shajahan et al. 2017). However, this process is time-consuming, labor intensive, and easy to make errors due to visual fatigue (Shajahan et al. 2017). Thus, digital imaging and computer vision could be a reliable alternative for manual pest monitoring and counting (Shajahan et al. 2017).

Lastly, the quality of agricultural produce has been graded by human inspection based on color, texture, and size (Sahitya et al. 2021). This inspection process is tedious, time consuming, and costly, which could cause delay in transportation (Sahitya et al. 2021). Image analysis algorithms to classify fruit and extract key features such as size, color, texture, and shape could aid processing plants in efficiently sorting for quality

produce (Sahitya et al. 2021). These image analysis techniques require extra steps of machine learning based on convolutional neural network (CNN) (Sahitya et al. 2021) or other type of neural network analysis (Rafiq et al. 2016). Rafiq et al. (2016) provided examples of grading the quality of tomatoes based on color and size to classify the ripening stage. The objective for this chapter is to broaden the understanding of image analysis used in different areas of agriculture areas including: 1) leaf damage symptoms, 2) stress evaluation, 3) plant growth evaluation, 4) stand/insect counting, and 5) evaluation for produce quality.

### **Quantifying Leaf Damage Symptoms**

In general, leaf damage symptoms can result from plant diseases, pest infestation, nutrient deficiencies or toxicities, and even certain herbicide injury. Plant disease is a major threat for the agriculture industry, thus, early detection with a proper treatment plan is crucial to prevent significant yield reduction. In addition, being able to quantify disease is important for determining crop loss, establishing disease thresholds for decision making, improving knowledge for disease epidemiology, and evaluating the effect of pesticide treatments or cultivar differences in host-plant resistance (Chaimala et al. 2020).

#### ***Visual Rating of Leaf Damage***

Identification of crop diseases and quantifying disease severity are usually done by highly trained experts through visual examination, and these experts often rely on their knowledge and experience (Singh et al. 2020). Rating for disease severity level is a hard task and usually time consuming. Even with proper training, raters cannot avoid bias that can lead to variable results (Stewart and McDonald 2014). Bock et al. (2009) conducted

citrus canker foliar symptoms assessment comparing 28 human raters (experienced and inexperienced) with standardized image analysis using two hundred digital leaf images ranging from 0-37% infected area. Results showed researchers overestimated percent necrotic area (%N), and percent chlorotic + percent necrotic area (%CN) when there were more lesion numbers on the leaves. However, the average from the 28 rates was close to the actual ratings determined from image analysis. Visible imaging and hyperspectral imaging on the other hand are highly reliable especially under controlled conditions (Bock et al. 2020). Sarkar et al. (2021) also demonstrated that visual ratings could not avoid personal scoring bias when selecting drought tolerance peanut lines from thousands of the breeding lines.

For disease visual grading, the use of standard area diagrams (SAD) has shown improved accuracy and reliability. For SAD, a set of illustrations is used to demonstrate incremental percent severity values (Nutter et al. 1993). The SADs are designed to aid raters to accurately interpolate the percent severity between the guide reference pair most closely resembling the specimen in question (James 1971). Domiciano et al. (2013) designed SAD sets that included images of wheat leaves with distinct disease severities (0-1, 1, 5, 10, 20, 30, 40, 50, 60, 70, and 83%) of spot blotch (Figure 2.1(a)). Results from 12 raters without experience in evaluating plant disease showed improved accuracy and reliability in estimating spot blotch severity on wheat leaves. Similar research using SADs was done on soybean rust (Franceschi et al. 2020) (Figure 2.1(b)), bacteria spot on tomatoes (Duan et al. 2015) (Figure 2.1(c)), and bacterial blight on eucalyptus trees (Borges et al. 2020) (Figure 2.1(d)). All showed improved accuracy and reliability for inexperienced raters who used SADs when rating for disease severity.

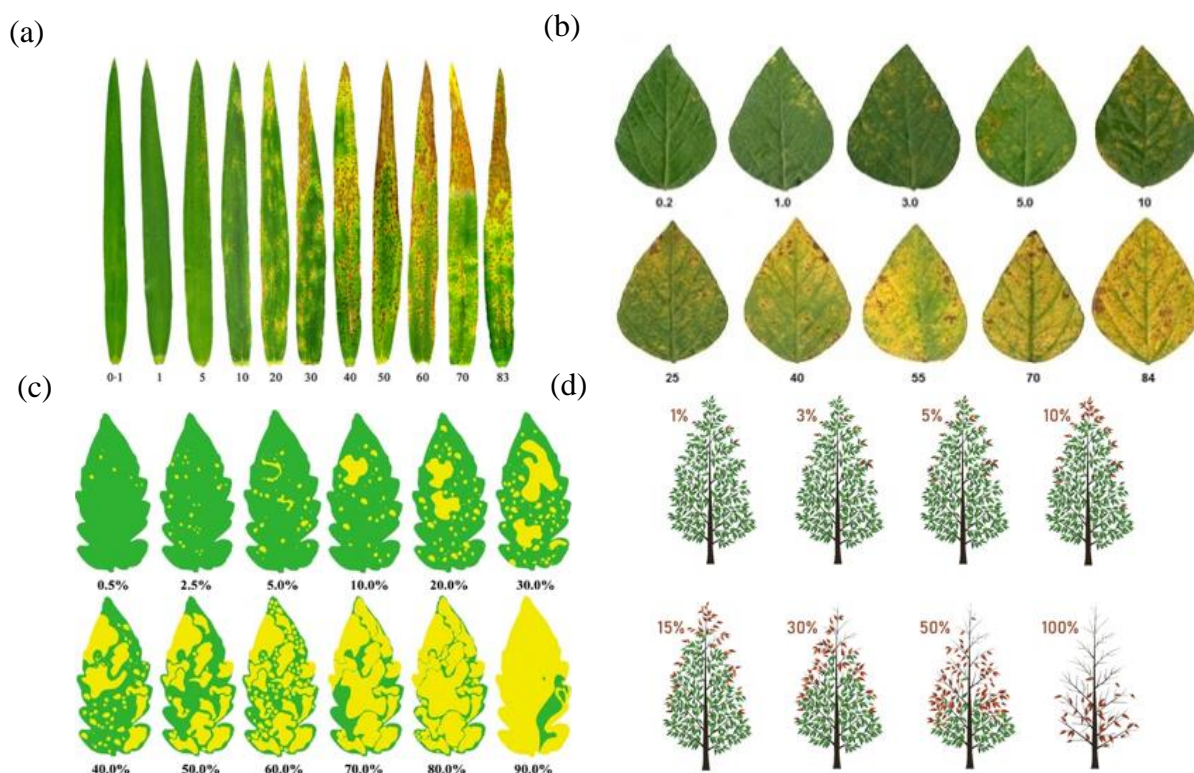


**Figure 2.1.** Standard area diagrams (SAD) for accessing different plant diseases: (a) Spot blotch severity on wheat leaves (figure source Domiciano et al. 2013); (b) Rust (*Phakopsora pachyrhizi*) severity on soybean (*Glycine max*) leaves (figure source Franceschi et al. 2020); (c) Disease severity estimation of *Xanthomonas euvesicatoria* race T1 on tomato leaves (figure source Duan et al. 2015); (d) Bacterial blight (*Erwinia psidii*) severity on eucalyptus trees (*Eucalyptus grancam* × *Eucalyptus urophylla*) (figure source Borges et al. 2020).

### ***RGB Imaging for Leaf Damage Estimation***

Image analysis can be applied to analyze reflectance in the visible spectrum for plant disease. Visible spectrum image analysis is usually done by measuring the number of pixels that are pre-defined as diseased compared with pixels that are pre-defined as healthy (Bock et al. 2020). Custom systems using color transformation are the simplest methods for visual image analysis. For analysis, the first step is to create a binary mask to remove background, use color segmentation to isolate regions of interest, and then use

algorithms to quantify disease symptoms. Contreras-Medina et al. (2012) used these methods to estimate common plant disease symptoms such as chlorosis, necrosis, leaf deformation and mosaics. They provided visualization of these symptoms on bean (*Phaseolus vulgaris*), pepper (*Capsicum annum*), and pumpkin plants (*Curcubita pepo*) (Figure 2.2-2.5). They also provide algorithms specific to quantify each symptom.

The algorithm used to quantify pumpkin chlorosis (Figure 2.2) is based on color analysis. The algorithm was separated into two stages. The first stage was to calculate the extent of yellowing of the leaf. Then, the image was sectioned into four and the average yellowing of the four sections was calculated. This established whether the chlorosis was generalized or localized.

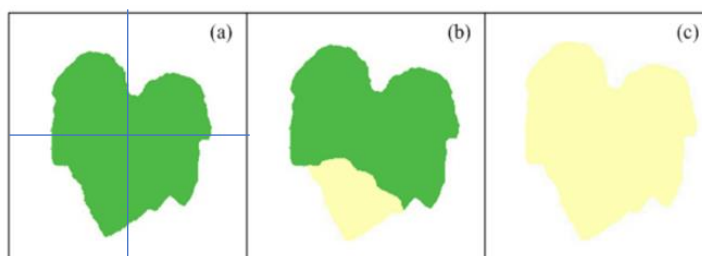


**Figure 2.2.** Visualization of chlorosis on a pumpkin leaf: a) healthy leaf with homogeneous green color; b) pumpkin leaf with localized chlorosis; c) pumpkin leaf with generalized chlorosis (figure source Contreras-Medina et al. 2012).

The algorithm for necrosis (Figure 2.3) was also based on color analysis by using the green and blue components of the RGB image. The green component is used to isolate the necrotic area of the leaves because it provides a good color contrast between necrotic and non-necrotic tissues. The blue component is utilized to calculate the total leaf area because it is less sensitive to symptoms such as chlorosis and offers a better differentiation of leaf from the background.

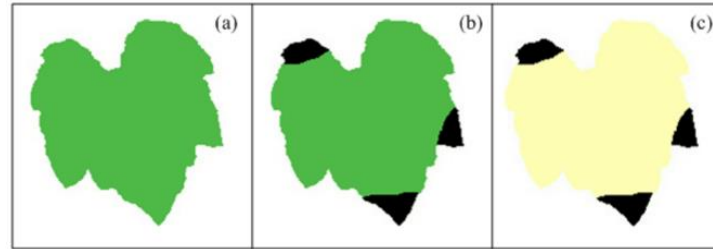


**Figure 2.3.** Visualization of necrosis on pumpkin leaf: a) healthy leaf with homogeneous green color; b) non-chlorotic pumpkins leaf with necrotic areas (black); c) chlorotic pumpkin leaf with necrotic areas (figure source Contreras-Medina et al. 2012).

The presence of leaf deformations can also be determined by using RGB image analysis (Figure 2.4). The symptoms usually show changes in the shape or form of the plant leaf with twisted, deformed, or distorted leaves. This can be caused by plant pathogens, mineral nutrition deficiencies, insect feeding, or herbicide injuries. Figure 2.4 shows the contours of pepper leaves that range from healthy (a) to severely deformed (c).

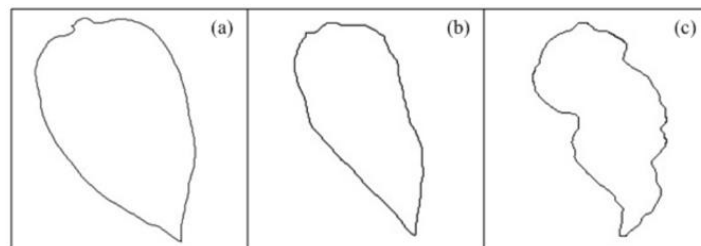


**Figure 2.4.** Leaf deformation symptom: a) healthy pepper leaf with no deformations; b) pepper leaf with few deformations; c) pepper leaf with severe deformation (figure source Contreras-Medina et al. 2012).

Evaluation of leaf deformation used a color-based algorithm that involved the blue component described previously as it is less sensitive to other symptoms that could add error in quantifications. The sphericity index from Pratt (2001) enabled quantification of the shape of an object. The formula requires measurement of leaf area ( $A$ ) and the

perimeter of the leaf ( $p$ ). The deformation index ( $I$ ) can then be calculated based on the Pratt (2001) formula:

$$I = \frac{p^2}{4\pi A}$$

After calculating the deformation index, the value of healthy and unhealthy (deformed) leaves can be quantified and compared for the severity of deformation.

The mosaic algorithm is based on the extent of leaf venation (Figure 2.5). It is assumed that severe mosaic symptoms will have greater leaf venation, and this can be quantified by using edge detection to measure the extent of leaf venation. The blue component will be used as it is better able to represent leaf area. However, this will require having light shining from the back of the leaves to more clearly capture leaf venations.

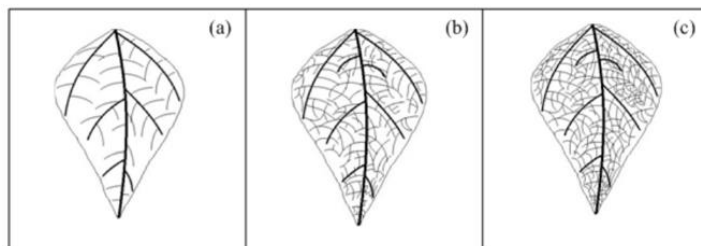


**Figure 2.5.** Mosaic symptom generally caused by plant viruses. (a) healthy bean leaf with no mosaic symptom. (b) unhealthy bean leaf with low density mosaic symptom. (c) unhealthy bean leaf with high density of mosaic symptoms (figure source Contreras-Medina et al. 2012).

### *Using Spectral Sensors for Disease Identification*

Multispectral and hyperspectral imaging allows capturing wavelengths beyond the capability of typical RGB cameras. Hyperspectral cameras can assess narrow wavelengths in the visible spectrum from 400-700 nm, near-infrared (NIR) range from 700 to 1,000 nm, and the shortwave infrared wavelengths range from 1,000 to 2,500 nm

(Mahlein et al. 2018). Multispectral cameras are not as complex and sophisticated and cover a much more restricted range of wavelengths most often in the RGB and NIR ranges. However, both are capable of detecting differences in plant reflectance and identifying plant disease. For disease detection, the visible and near infrared regions (400–1000 nm) provide the most reflectance information (Bock et al. 2020).

The optical properties of leaves are determined by: 1) light transmitted through the leaf, 2) light absorbed by the leaf as impacted by leaf structures and chemical makeup (e.g.; pigment, water, sugar, lignin, and amino acid content), and 3) light reflected directly from leaf surface or reflected from internal leaf structures (Mahlein 2016) (Figure 2.6(a)). The visible range is characterized by strong absorption of light by photosynthetic pigments in a green leaf. The optical properties at the infrared range are affected by leaf cellular structure and internal structure (fraction of air spaces) (Carter and Knapp 2001, Jacquemoud and Ustin 2001). The shortwave infrared range is sensitive to water content and the composition of leaf chemicals in leaves such as chlorophyll and dry matter when the leaf wilts (Carter and Knapp 2001, Jacquemoud and Ustin 2001). Mahlein (2016) demonstrated changes in reflectance from leaves can result from the development of plant pathogens. These changes were explained by highly specific impairments in leaf structure and chemical composition such as chlorophyll, toxins, and degradation enzymes of the leaf tissue during the pathogenesis of powdery mildew, rust, and leaf spots (Figure 2.6(b)). Biotrophic fungi such as powdery mildew and rust have little impact on tissue structure and chlorophyll composition during the early infection stages. However, later in disease development both powdery mildew and rust produce fungal structures on the leaf surface that influence the optical properties of the plant

(Mahlein 2016). Perthotrophic pathogens that cause leaf spots often induce degradation of tissue due to pathogen specific toxins or enzymes that cause necrotic lesions (Mahlein 2016).

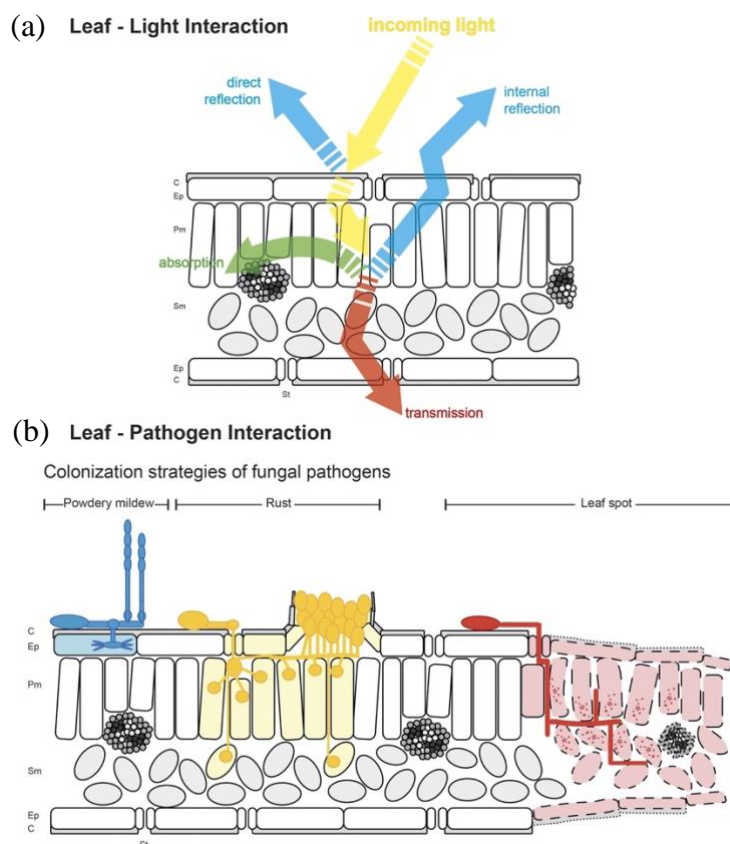


**Figure 2.6.** (a) The interaction between light and leaf depending on leaf structural and chemical properties; (b) Disease infection can alter leaf structural and chemical properties (figure source Mahlein 2016).

Unique spectral signatures related to specific disease can be detected by measuring reflectance wavelength patterns with a hyperspectral camera. Wahabzada et al. (2015) provided examples of using hyperspectral imaging to differentiate barley disease net blotch, rust, and powdery mildew (Figure 2.7). Creating archetypal signatures that extract disease specific spectral signatures over time, allow for better differentiation

between different developing stages of the diseases (Wahabzada et al. 2015). By using Metro Maps based on the hyperspectral dynamics, Wahabzada et al. (2015) demonstrated disease progress under different wavelengths such as visible near infrared (VNIR) and short-wave infrared (SWIR). Separation can be clearly seen in the VNIR region for net blotch, rust, and powdery mildew and net blotch can be easily separated in the SWIR region (Figure 2.8).

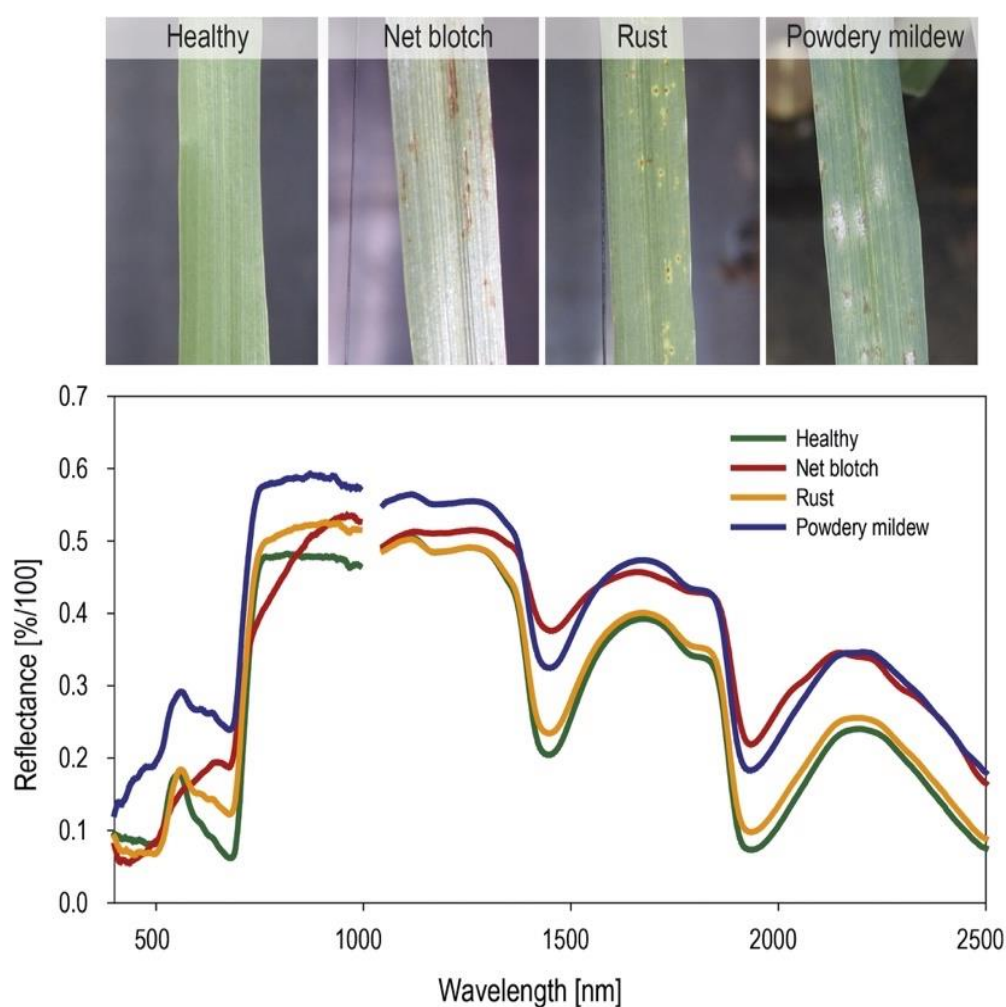


**Figure 2.7.** Spectral signature of barley leaf disease net blotch, rust, and powdery mildew (figure source Wahabzada et al. 2015).

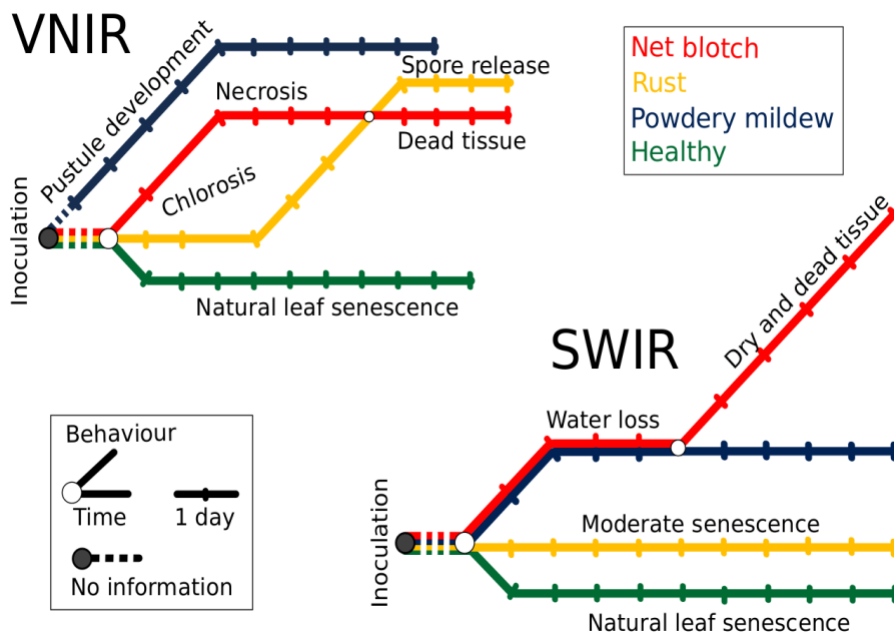


**Figure 2.8.** Disease progression via Metro Maps of hyperspectral dynamics. Barley leaf disease net blotch, rust, powdery mildew can be clearly separate based on signature wave band in the VNIR and SWIR region (figure source Wahabzada et al. 2015).

Rumpf et al. (2010) used hyperspectral data to detect cercospora leaf spot, leaf rust, and powdery mildew disease on sugar beets even before the symptoms appears. This is done by inoculating sugar beets with each disease and measuring wavelength from 400 to 1000nm at different times until 20 days after the inoculation. Support Vector Machine was used to classify each wavelength corresponding to each different disease. Support Vector Machine is a powerful classification method based on statistical learning theory (Vapnik 1998). In general, classification algorithm finds patterns in empirical data and classifies them into different classes (Rumpf et al. 2010). Apan et al. (2004) demonstrated Hyperion imagery can detect orange rust disease in sugarcane crops. The Hyperion sensor is carried by the National Aeronautics and Space Administration (NASA) Earth Observing 1 satellite (Ungar 2001). It is the first spaceborne hyperspectral instrument to

acquire both visible near infrared (VNIR 400-1000 nm) and shortwave infrared (SWIR 900-2500 nm) spectra. Hyperion images 256 pixels with a nominal resolution of 30 m on the ground over a 7.65-km swath (Datt et al. 2003). Apan et al. (2004) showed the combination of the visible near-infrared bands and the moisture-sensitive short-wave infrared band (1660 nm) increased the separability of rust-affected areas.

### **Stress Detection Through Imaging Analysis**

Crop yields rely on a suitable environment and growing conditions. Under prolonged stress, crop growth and yield will be compromised (Gaspar et al. 2002). In the United States, some major crops including corn, wheat, soybean, sorghum and oats only achieved 22% of their genetic potential yield due to unsuitable growing conditions (Boyer 1982, Taiz et al. 2015). Breeding and better crop management will enhance crop productivity for growers. In addition, global warming, climate change, and industrial pollution could intensify plant stress and affect crop productivity. Image analysis can be used to measure the severity of different stresses. For water stress, hyperspectral or thermal sensors can visualize the stress levels and be used for efficient irrigation scheduling. In this section, we will explore how image analysis can be applied in different scenarios to detect stresses.

#### ***Detecting Iron Deficiency with RGB Imaging***

Soybean is an important row crop in the U.S. But iron deficiency chlorosis is a yield-limiting abiotic stress that is common on calcareous soils with high pH (Naik et al. 2017). Naik et al. (2017) used RGB image analysis to evaluate soybean iron deficiency severity. This image analysis followed the following framework: 1) image acquisition, 2) image processing, 3) feature extraction, and 4) classification and machine learning. For

image acquisition, images were taken using Canon EOS REBEL T5i camera, and the whole canopy was included in the field of view of the camera. Image processing included three steps. First, white balance and color calibration were applied to ensure color uniformity for all the images collected. Then, segmentation was used to crop out the soybean plant from the background by removing pixels that were neither green nor brown. Lastly, noise and outlier removal were done to remove things like plant debris and soil from the image. Feature extraction was based on the color signatures (e.g., chlorosis is yellow; necrosis is brown) (Figure 2.9). Each pixel of the processed image belonging to the canopy was classified as either green, yellow, or brown. For each image, the percentage yellow (%Y) is calculated as  $\%Y = (\text{Area of yellow}) / (\text{Area of total}) * 100$  and percentage brown (%B) is calculated as  $\%B = (\text{Area of brown}) / (\text{Area of total}) * 100$ . Then a rating scale of 1-5 for iron deficiency chlorosis was established based on the %B on the leaves (Figure 2.10).

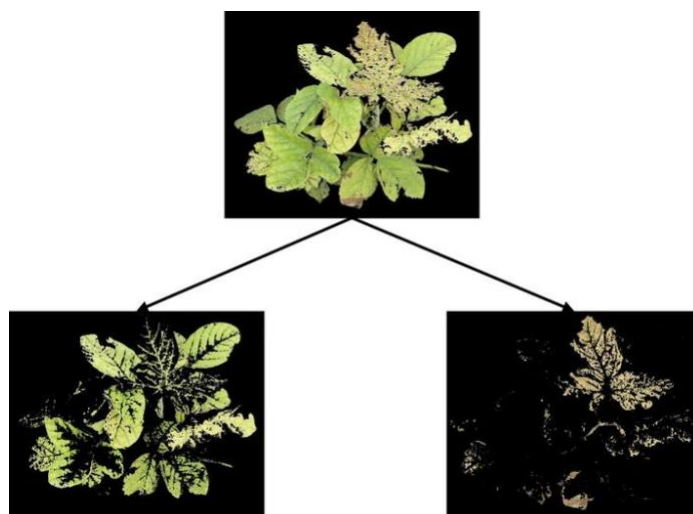


**Figure 2.9.** Feature extraction of soybean plants with iron deficiency chlorosis (top). The bottom left image represents leaf areas yellow in color. The bottom right image represents leaf areas brown in color (figure source Naik et al. 2017).

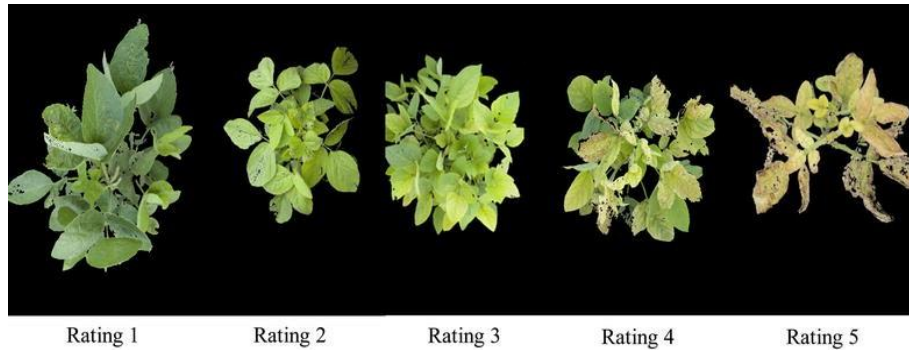


**Figure 2.10.** Iron deficiency chlorosis severity visual rating scale from 1-5 (figure source Naik et al. 2017).

Ten different classification algorithms were used in rating iron deficiency chlorosis including decision trees, random forests, naïve bayes, linear discriminant analysis, quadratic discriminant analysis, support vector machine, k-nearest neighbors, gaussian mixture model, and hierarchical classification. Results showed the best classifier to be the hierarchical classifier that produced a mean accuracy of approximately 96%.

### ***Drought Stress Detection***

Plant phenotyping can be used to contrast genotypes that are tolerant to drought stress. Casari et al. (2019) used thermal and RGB cameras to identify corn genotypes with drought tolerance. Both thermal and RGB images were taken at different time intervals by using a UAV. Thermograms displayed temperature distribution in the maize canopies, and the RGB images enabled extraction of plant leaf pixels to identify plant pixels in the thermograms (Figure 2.11). For maize, studies have shown drought tolerant genotypes have lower canopy temperatures likely due to its higher stomatal conductance to cool down plants (Romano et al. 2011, Zia et al. 2013). The frequency histogram of the canopy pixel temperatures can be segmented and extracted based on thermal images and

then used to compare corn genotypes for drought tolerance (Figure 2.12). Based on thermal and RGB images, Casari et al. (2019) was able to select corn genotypes with drought tolerance that are better than the traditional phenotyping by visual examination. This research indicates thermography may be applied to screening maize lines for drought tolerance (Casari et al. 2019).

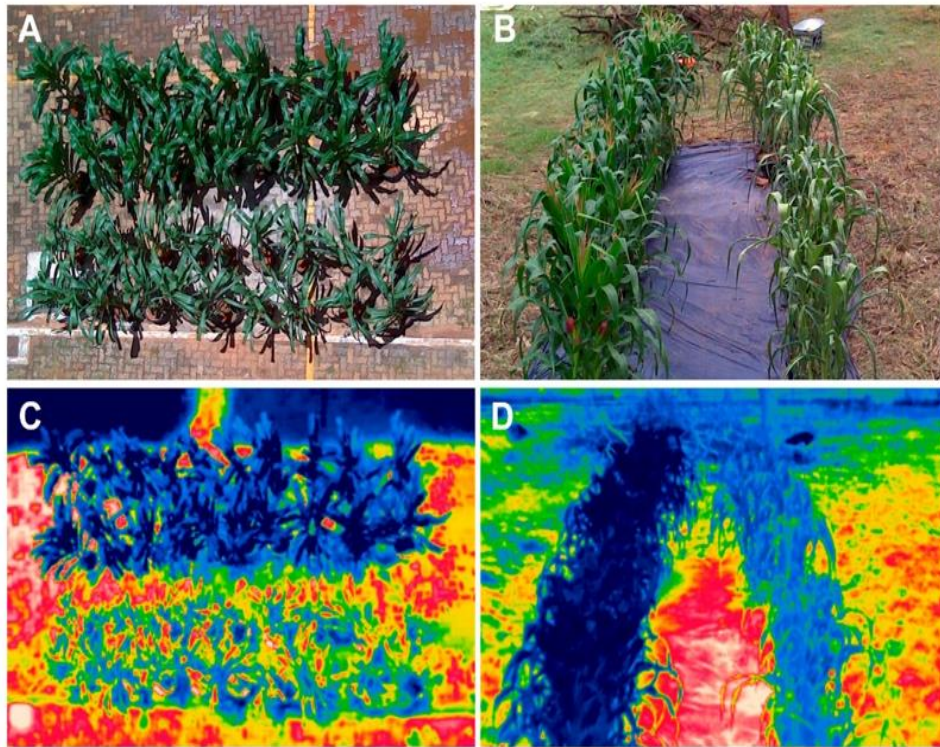


**Figure 2.11.** RGB (A, B) and thermal images (C, D) of drought stressed maize. Top row (A, C) and left row (B, D) of maize are drought tolerant (figure source Casari et al. 2019).

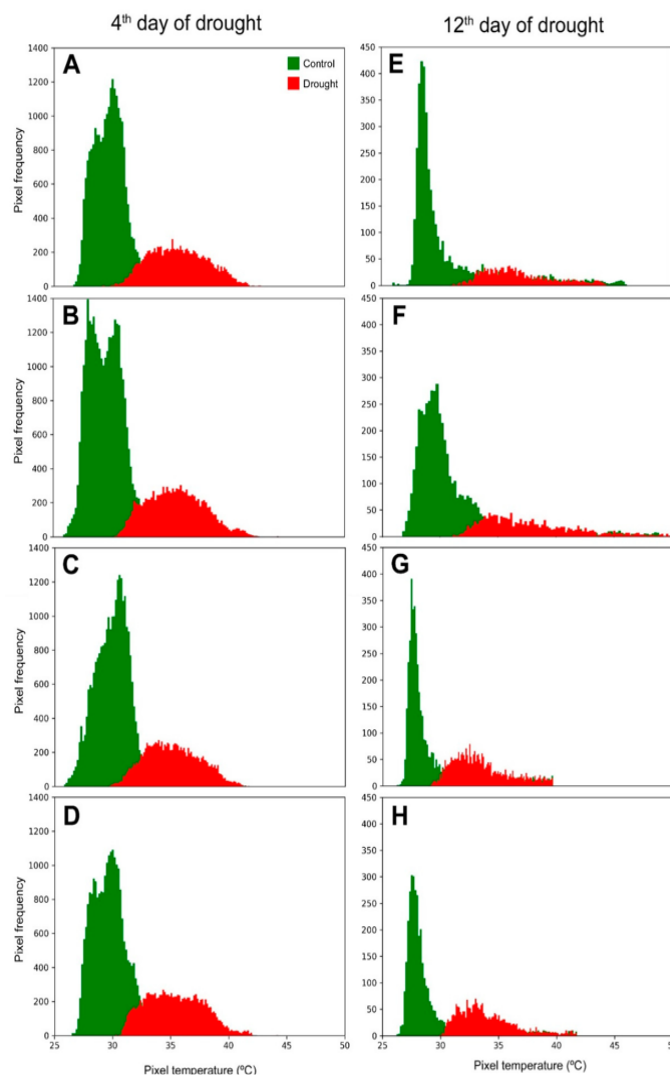


**Figure 2.12.** Frequency histograms of canopy temperatures for control and drought stressed maize plant. Four different varieties were compared at both 4<sup>th</sup> day (A-D) of drought and 12<sup>th</sup> day of drought (E-H). Better separation can be seen at the 12<sup>th</sup> day of drought where F is the least drought tolerance and G is the most drought tolerance (figure source Casari et al. 2019).

Simplex volume maximization (SiVM) is another technique that has gained popularity in early detection for drought stress. This technique is done by using data clustering to automatically evaluate hyperspectral signatures (Thureau et al. 2010). The algorithm allows fast calculation of massive datasets, and it calculates how similar each spectrum is to the already defined healthy or stressed spectral signatures. Spectral

signatures from healthy and stressed plants were clustered into those two classes. When measuring spectral reflectance from new samples, similar signatures were classified based on the pre-learned sample signature (Lowe et al. 2017). Römer et al. (2012) used the SiVM technique to test drought stress on potted barley plants and corn plots. By comparing this method with the well-known vegetation indices such as Normalized Difference Vegetation Index (NDVI), photochemical reflectance index, red edge inflection point index, and carotenoid reflectance index, SiVM was able to detect early drought stress more effectively even though the effects on leaf and canopy reflectance were subtle. NDVI is highly correlated to green-leaf density and vigor, and it is generally used as a proxy for the status of aboveground biomass (Ji and Peters 2003).

Photochemical reflectance index is derived from narrow-band spectroradiometers, and it is commonly used as an indicator of photosynthetic efficiency (Garbulsky et al. 2011).

Chlorophylls and carotenoids are the main pigments of green leaves, and they are important for photosynthesis in plant (Gitelson et al. 2002). Red edge inflection point index is widely used to estimate chlorophyll concentrations (Gitelson et al. 2002). The carotenoid reflectance index is widely used to estimate carotenoid concentrations in the plant (Gitelson et al. 2002). All of these can be used to indirectly observe plant water status.

### ***Salt Stress Detection***

The soil salinity issue is one of the major limitations affecting crop productivity worldwide (Yang and Yen 2002). High salinity can stunt plant growth by reducing cell expansion, decreasing protein synthesis, and accelerating cell death (Yang and Yen

2002). Hyperspectral imaging techniques have been extensively used to reveal levels of salinity in soil and canopy by measuring the spectral reflectance (Sytar et al. 2017). In hyperspectral imagery, mixed pixels are a result of mixture of more than one distinct substance. This could be due to low spatial resolution that disparate material can jointly occupy a single pixel or distinct materials are combined into a homogeneous mixture (Keshava and Mustard 2002). Spectral unmixing is the process of decomposing the spectral signature of a mixed pixel into their corresponding components (Shi and Wang 2014). These pure spectral signatures are called endmembers (Garg 2020). By doing spectral unmixing using hyperspectral imaging from the soil, it was found saline endmembers showed higher reflectance at 800nm, and broad absorption at 1450 and 1900nm (Sytar et al. 2017). These spectral signatures are useful for mapping fields with high salinity. Lara et al. (2016) used hyperspectral imaging to evaluate water salinity effects on lettuce. At different salinity levels, three wavelengths in visible and red edge regions (675, 710 and 745 nm) consistently demonstrated the salinity effect on lettuce leaves. Thus, the author proposed the level salinity index (LSI) to quantify the salinity stress on plant ( $LSI = [(R_{675} + R_{745})/2] - R_{710}$ ). This index-based model is simple and easier to apply and allows implementation with less expensive multispectral devices (Lara et al. 2016).

The ultraviolet (UV) range (200–380 nm) has also been investigated in efforts to detect plant salt stress. A few works have shown plant molecules such as flavonoids and phenolic compounds have better absorption in the UV range (Bhattacharya et al. 2010, Giusti et al. 2014). A previous study has shown barley seedlings under salt stress have increased flavonoids and total phenolic compounds (Ali and Abbas 2003). Brugger et al.

(2019) demonstrated the first research using hyperspectral sensors that focus on the UV range to detect salt stress in barley. Plants under biotic stress have characteristic spectral signatures in the UV-range that are able to establish correlations to secondary plant metabolites (e.g., flavonoids and total phenolic compounds) (Brugger et al. 2019). This allows detection of salt stress. However, there are constraints to generating quality data in the lower spectral regions. This is due to overlapping spectral signatures that make it hard to quantify the specific plant molecules.

### **Plant Growth (Vigor) Evaluation**

Plant growth (vigor) can be a useful indicator to justify the efficiency of using fertilizer and irrigation and the positive or negative impacts of other agricultural inputs (growth regulators, pesticides, etc.). Additionally, measuring plant growth can provide plant breeders phenotype data for selecting superior genotypes. Image analysis using RGB cameras or spectral sensors can provide effective and efficient measurement of plant vigor and growth.

#### ***RGB Imaging***

The simplest measure of plant growth from RGB images is measuring the green pixels (i.e., the plant) relative to the background (soil, fabric, container, etc.) (Paruelo et al. 2000, Stewart et al. 2007). RGB images can be taken by digital cameras or smart phones, and image analysis can be done on ImageJ (an open resource software).

On ImageJ, the key for image analysis is to select the correct color threshold to separate the plant from the background and then create a binary mask of the plant (Agehara 2020) (Figure 2.13). Non-target plants (i.e., weeds) present in the photo can be

removed using the paintbrush tool in ImageJ. At the end, those green pixels can be analyzed and quantify as area. Area change at different times can then represent growth or percentage growth.



**Figure 2.13.** Overhead canopy images of various crops converted to binary images using ImageJ for canopy cover measurement (figure source Agehara 2020).

The key to obtaining effective images for analysis and comparison is to always set the camera at same height and location relative to the target when taking images at different times. When taking pictures in the field, variable lighting conditions can shade parts of the plant canopy and make it hard to include coverage of the entire plant. This requires the use of software such as Adobe Lightroom to enhance the colors so all the green pixels can be detected in the image analysis.

Canopeo is the mobile smart phone application that was developed in the MATLAB programming language (Mathworks, Inc., Natick, MA) and uses RGB color values (Patrignani and Ochsner 2015). The analysis is based on the selection of the pixel ratios of R/G, B/G (Liang et al. 2012, Paruelo et al. 2000) and the excess green index (Chen et al. 2010, Richardson et al. 2007). The excess green index contrasts the green

portion of the spectrum against red and blue to distinguish vegetation from soil (Komarkova et al. 2020). The formula for excess green index is  $(2 \cdot G - (R+B))$  (Larrinaga and Brotons 2019). The image analysis uses these selected pixels to create a binary mask to measure the area covered by the plant. Canopeo also has the capability to reduce noise by removing isolated green pixels. In addition, Canopeo can detect all green parts of plants exposed to sunlight, and a great portion of shaded leaves. SamplePoint is a manual pixel classification program developed by Booth et al. (2006), and it is often used for field ground cover measurement. The pixel-level accuracy of Canopeo was evaluated by using SamplePoint as the “gold standard” (i.e., best available benchmark). Patrignani and Ochsner (2015) showed Canopeo correctly classified 90% of pixels of what is classified by SamplePoint. However, Canopeo’s image processing speed was 75 to 2500 times faster than SamplePoint.

### ***Spectroradiometer Imaging***

Spectroradiometers provides fast and non-destructive estimations of green biomass and chlorophyll content at canopy level (Aparicio et al. 2000). However, most of them are expensive and usually only carry passive sensors (i.e., depends on external source such as sunlight) (Cabrera-Bosquet et al. 2011). Until recently, the cost effective and easy to handle spectroradiometers such as GreenSeeker™ (NTech Industries Inc., Ukiah, California, USA) with active sensors (i.e., carries its own light source) have been widely adopted to measure plant growth in the field. The GreenSeeker™ has an integrated optical sensor that uses light emitting diodes (LED) to generate red and near infrared (NIR) light and measures reflected wavelengths that enable calculation of the normalized

difference vegetation index (NDVI). Computation of NDVI measures the differences between NIR (770nmλ) and red reflectance region (660 nmλ) using the formula:

$$\text{NDVI} = \frac{(\text{NIR} - \text{RED})}{(\text{NIR} + \text{RED})}$$

NDVI values represent absorption of red light by plant chlorophyll and the reflectance of NIR by water filled leaf cells (Govaerts and Verhulst 2010). NDVI has proven very useful because it correlates positively with intercepted photosynthetically active radiation and the nitrogen content in plants (Chen and Brutsaert 1998). Because of this, NDVI measured by handheld spectroradiometers can provide good representation of plant growth especially in small plot studies measuring the same plot at different time points. From personal research experience at RD4AG, measuring NDVI using GreenSeeker™ is a good indicator of plant growth (vigor), especially with fertilizer studies using different levels of nitrogen. NDVI can also be a good indicator when working with herbicide injury (pre-post emergence) by measuring the greenness of small plots.

### **Image Analysis for Counting**

Counting is often important in agricultural research. Counting insects is crucial in developing and using economic injury levels and economic thresholds. It is also a common method to estimate pesticide efficacy. Plant stand counts are important for breeder to evaluate plant emergence and estimate uniformity. All of these were traditionally done by manually counting, but this is labor intensive, time consuming, and increases the chance to make mistakes. Thus, image analysis methods were explored to improve counting accuracy and speed.

### *Insect Counting*

Insect counting is a common method used for evaluating pesticide efficacy. Research Designed for Agriculture (RD4AG) is a commercial contract research company located in Yuma, AZ, U.S. that undertakes numerous pesticide efficacy trials. The company developed an efficient method for counting whiteflies after the application of different pesticides. Leaf disks were collected from treatment plants at different time points by using leaf punches (MIDCO Global, Kirkwood, MO, United States) with ½” disk size (1.27cm). The punched leaf tissues were collected into a 50 ml centrifuge tube that was labeled corresponding to the plot number, kept in an ice chest, and carried back to the office for counting. Whitefly nymphs and eggs were counted on the underside of the leaf because that is where whiteflies generally lay eggs. The process requires experienced technicians to count under the microscope, but the process is very tiring and time consuming. To improve the process, Connor Osgood (Research Agronomist II) came up with the idea of using a printer scanner to scan multiple leaf disks to create a digital image with high resolution. This enabled counters to do the counting at their own comfort and pace without the use of microscopes. This creates a backup for checking the counting, but it also provides flexibility in scheduling since leaf disks will deteriorate if kept in the refrigerator for more than 2 days.

The imaging process is done by using Epson Perfection V370 photo scanners (Seiko Epson Co., Nagano, Japan) that connected into a computer. The punches from each plot are placed onto a predefined grid on the scanner glass and a plot ID label is made visible in the image (Figure 2.14).

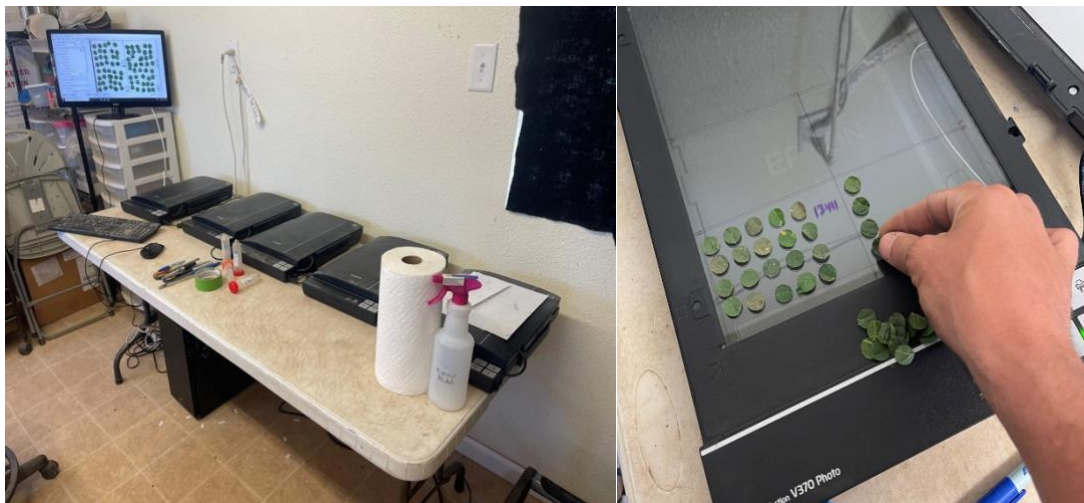


**Figure 2.14.** Scanning set up using Epson Perfection V370 photo scanner. Figure on the left is the working station using up to 5 scanners at one time. Figure on the right is the demonstration of the predefined grid on the scanner glass with plot ID labeled (figure credit: Connor Osgood).

Images are then scanned at a high resolution of 4,800 pixels-per-inch. The scanned image can be saved as an unedited raw TIFF, or JPEG. Each scanner can scan 8 plots worth of leaf disks (20 disks per plot). Scanning at high resolution made is easy for raters to identify whiteflies eggs and nymphs, but it also creates massive files around 250Mb for an image including 8 plots (Figure 2.15).



**Figure 2.15.** Figure on the left showed an example of a scanned image including 8 plots of disks. Figure on the right showed the high resolution made is easy to identify nymphs and eggs (figure credit: Connor Osgood).

To separate the large image into separate plots, ImageJ has the built-in feature for splitting images into equal squares which can break the big 250Mb size into smaller (18-30) Mb for individual plot images. This splitting process can be done using the macro function in ImageJ and running on batch to split automatically (Figure 2.16).

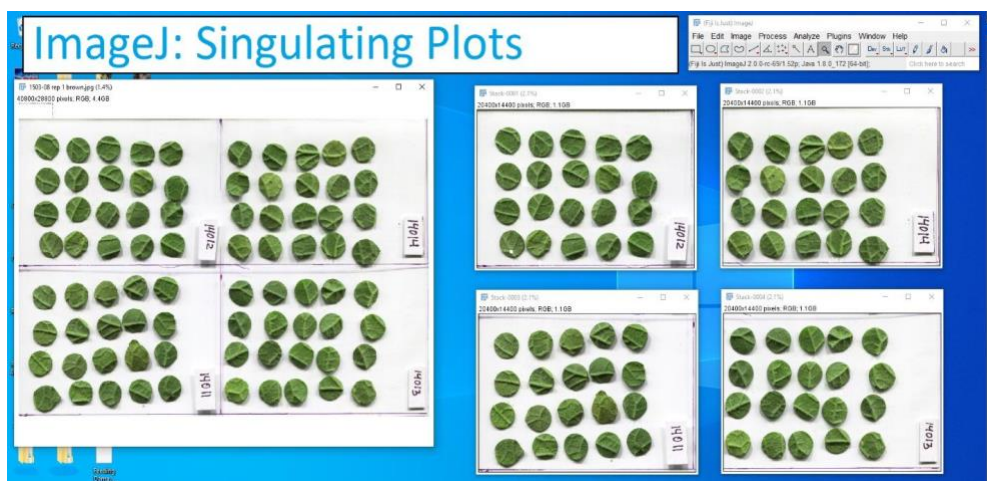


**Figure 2.16.** The splitting processes using ImageJ to split an image to equal squares (figure credit: Connor Osgood).

This counting process is a rudimentary example with minimal use of image analysis, but it does demonstrate the advantages of imaging. Using the scanner method can reduce labor needs by about 50%. In the future, machine learning can be used to identify and count nymphs and eggs.

### ***Insect Counting Using Machine Learning***

The black pine bast scale (*Matsucoccus thunbergianae*) is a serious pest that causes widespread damage to black pine (Choi et al. 2019, Hong et al. 2021). Monitoring the occurrence and the population of *M. thunbergianae* is done by employing pheromone traps. However, counting insects is labor intensive. Hong et al. (2021) tested the use of

deep learning counting algorithms for evaluating pheromone trap images. Pheromone traps were collected in the field and photographed in the laboratory. Convolutional neural networks have shown high performance for tasks such as classification, detection, and segmentation of objects in images (He et al. 2017, Krizhevsky et al. 2017, Simonyan and Zisserman 2015). The convolutional neural networks tested in Hong et al. (2021) were Faster R-CNN Resnet 101, EfficientDet D4/D0, Retinanet 50, and SSD Mobilenet v.2. The resolution for the image was 6000 X 4000 pixels, but the size of *M. thunbergianae* was only 60 X 60 pixels which can lead to a decrease in detection performance. Because the cropped image has a larger object size relative to the image size than the uncropped image, the detection performance can be increased by cropping. Thus, the entire 6000 X 4000 image was cropped into smaller windows under the condition of 12 X 8 and 6 X 4. The detector set included the training and validation set, and these were used for training object detection. Test sets were used for optimizing detection. The counting set was counted by a person skilled in counting and used for evaluating the counting accuracy of the detection model.

Under two cropping conditions, counting accuracy was estimated at 95% or more in most models. Common detection errors included false negatives and false positives (Figure 2.17). False negative errors were more common than false positive errors. False negatives were due to several insects overlapping, or the shape of the insect was unclear. This can be hard for even the trained expert to detect. False positives are due to counting a shape that was similar to *M. thunbergianae* or detecting a portion of the *M. thunbergianae*, such as a wing (Figure 2.17 (d)).

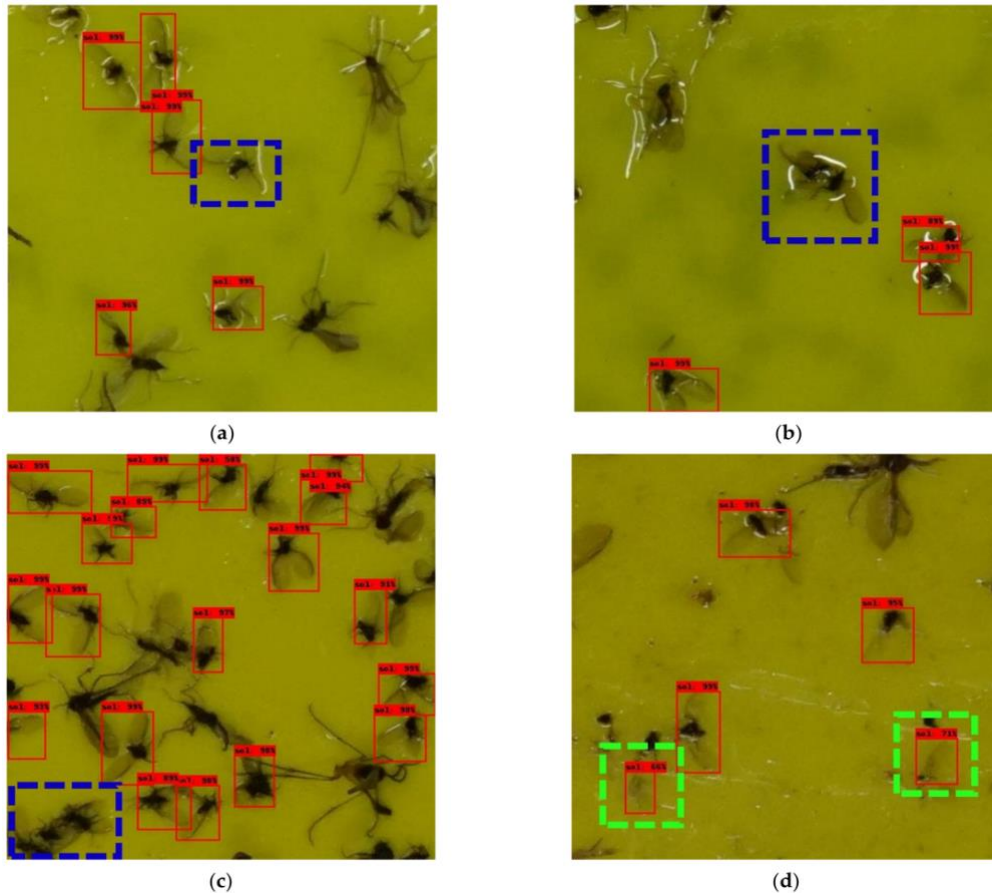


**Figure 2.17.** Detection errors found in convolutional neural networks. Box in red showed correct detection. The blue box in (a) to (c) were false negatives due to overlapping of insects or shape is unclear. (d) showed as false positive where wings were detected as *M. thunbergianae* (figure source Hong et al. 2021).

Similar research was done using convolutional neural networks that automatically segmented and counted aphid nymphs on Bok choy leaves (Chen et al. 2018). Automatic counting based on segmentation showed high precision (96%). The correlation between the automated and manual counting was high ( $R^2 = 0.99$ ). This showed that insect counting using convolutional neural networks can be applied for other species of pests.

### *Plant Stands Counts*

Plant stands counts are used to estimate emergence and plant uniformity. For farmers, early detection of uneven emergence can help make decisions for replanting (Shirzadifar et al. 2020). Image capturing devices such as unmanned aerial vehicles, high definition cameras, and even cell phone cameras offer new ways to collect information and use for analysis (Khaki et al. 2022). A recent study by Shirzadifar et al. (2020) used RGB images collected with unmanned aerial vehicles (UAV) to estimate corn stand count. This study did image mosaicking using AgiSoft PhotoScan™ software (AgiSoft LLC, St. Petersburg, Russia) to create an RGB image for the whole field. The image processing and analysis was done using MATLAB (Mathworks, MA, USA). Two image analysis methods were used to estimate corn stand count.

The first method used excess green or the excess green index. This was done with a simple algorithm that identifies green pixels (vegetation) in an image. Plant chlorophyll absorbs red and blue wavelengths but reflects the green component (Shirzadifar et al. 2020). The new grey scale image was constructed using the excess green index equation:

$$\text{Excess green index} = (2G - (R+B))$$

where pixel values range from 0 to 1. Plant pixels were equal or higher than an index of 0.2, and other objects (e.g., soil and residue) possessed index values less than 0.2. Based on their pixel values, plant pixels were segmented out from the background by creating a binary image. The morphological operation was then applied on the binary image to remove the noise around the plants. This is a function on MATLAB that remove the tiny objects by considering the pixels surrounding each pixel. The tiny objects will be

removed if the surrounding pixels did not have the same value. The label function on MATLAB numbered each object (plant) to count the total plant stand.

The second method used unsupervised machine learning with a k-means clustering-segmentation algorithms. The k-means clustering method divided objects into a specific number (k) of cluster groups by calculating and assigning each pixel to a specific cluster based on the similarity in pixel intensity. This separates pixels into different groups such as plants, bare soil, and residue. The morphological operation was also done in this method to remove the noise around the plants, and the label function was applied to perform the total plant stand count.

The results showed the k-means method had better accuracy at counting corn plants than the excess green index. The mean accuracy of the excess green index across three fields was around 46%, but the accuracy of k-means was around 91%.

### **Quality and Size Evaluation**

Agricultural produce such as vegetables and fruits require evaluation for quality and sorting for size before selling to the consumers. The efficiency and effectiveness of evaluation and sorting are important to ensure the quality standards which determine the marketability of the produce (Jarimopas and Jaisin 2008). Thus, having a rapid, consistent, effective, and robust method is necessary (Arjenaki et al. 2013). Issues related to grading include high labor costs, labor fatigue, inconsistency, and low precision. In addition, there are differences in personal perception of quality and scarcity of the trained labor to perform grading (Arjenaki et al. 2013). The key features inspectors are looking for include size, color, texture, shape, or wounding/injury on the surface. All the information can also be extracted by using image analysis and machine learning to

automate the evaluation processes. Machine learning can accurately identify the internal and external characteristics for agricultural produce including the degree of maturity, size, defects, moisture, and nutrients (Chen et al. 2002). This section will explore the application aspects of image analysis and machine learning.

### ***Surface Defect Detection and Grading***

Li et al. (2002) developed a computer imaging method to detect apple surface defects. The imaging system contained two CCD monochromatic cameras mounted above and below a conveyor in a lighting chamber. The conveyor was composed of fruit cups without bottoms. Two mirrors were fixed on both sides of the conveyor which allowed images to be taken on all four sides. The camera above the conveyor took three side views of an apple (top and two sides), and the camera below the conveyor took the bottom view of the apple. This imaging system was able to inspect multiple apples on the conveyor simultaneously on the four sides of each apple while it was traveling on the conveyor.

The algorithm developed for detecting surface defects included image processing, defect segmentation, stem-calyx recognition, and defect area calculation and grading. Image processing allowed the grader to remove the background. Apples are spherical in shape, and this results in changes of the image intensity across the apple. The changes of the image intensity caused the intensity values of the normal surface to be lower than the intensity of the defect on the surface of the fruit. Reference apple images were developed for defect segmentation. Subtracting the normalized testing image from the normalized reference image following threshold processing allowed easily extracting the defects.

During the defect inspection process, the stem and calyx can be mistaken as a defect. Thus, the stem-calyx concave area must be distinguished from the true defects. This process was achieved by fractal features and artificial neural network. After identifying the stem-end and calyx areas of the apple, defect areas were segmented and calculated for grading (Figure 2.18). The test results show that the accuracy of the network classifier was over 93%, proving its effectiveness. Similar evaluation for surface defects was also demonstrated on tomatoes by Arjenaki et al. 2013). This study used a different algorithm with detection accuracy of 84.4%.

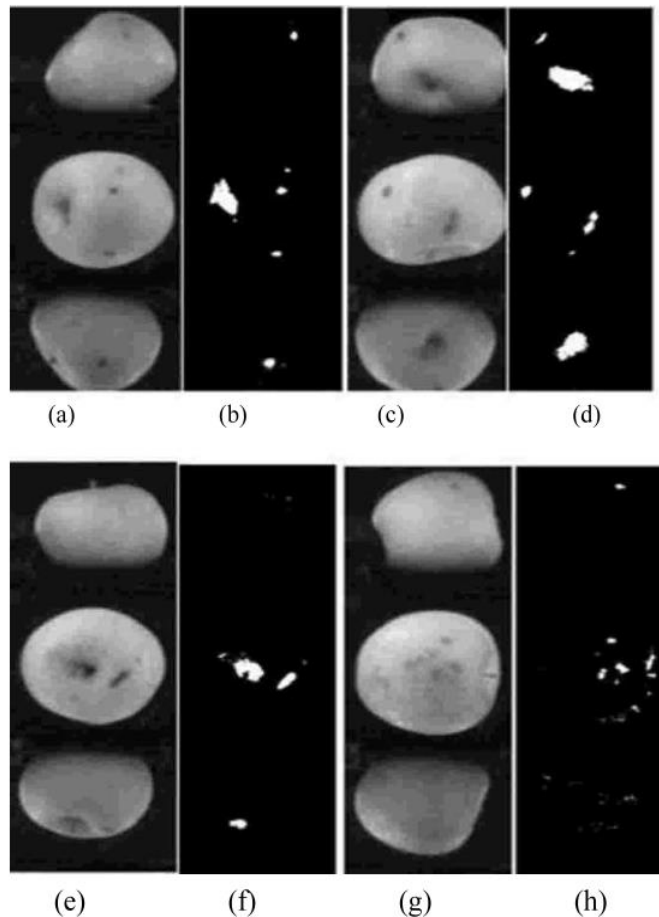


**Figure 2.18.** Defects segmentation. (a), (c), (e), and (g) were original images; (b), (d), (f), and (h) were segmented defects (figure source Li et al. 2002).

### *Sorting for Maturity and Size*

Fruits are generally sorted for quality and maturity level before transport to different standards of markets at different distance. This allows farmers to optimize profits. Color grading is often used by graders to sort for maturity (Lee et al. 2011). Shape is another common measurement used for produce quality evaluation. For example, fresh produce like potato needs to be uniform and regular in shape as well as free from defects to gain reasonable share in the highly competitive markets (ElMasry et al. 2012). Both color and size can be extracted from digital images, and this allows grading by using image analysis and machine learning.

Grading mango (*Mangifera indica L.*) quality involves evaluating color and size. Nandi et al. (2014) proposed an automated mango sorting and grading system consisting of a motor driven conveyer belt, image chamber with a light source supply, and CCD camera mounted on top. Images captured by the camera were evaluated by the color algorithm that automatically classified the fruit base color into four different maturity levels: raw (M1), semi-mature (M2), mature (M3), and over mature (M4). The sorting unit consists of four solenoid valves driven by respective drive units, that are controlled by the computer and sort mangos into appropriate bins. The authors used blue as the color of the conveyer belt because blue does not naturally occur in mangoes, and blue is one of the three channels in the RGB color model. This makes it easier to separate the background from the mango in the image. Five varieties of mango with different maturity levels (M1, M2, M3, and M4) are demonstrated in Figure 2.19.

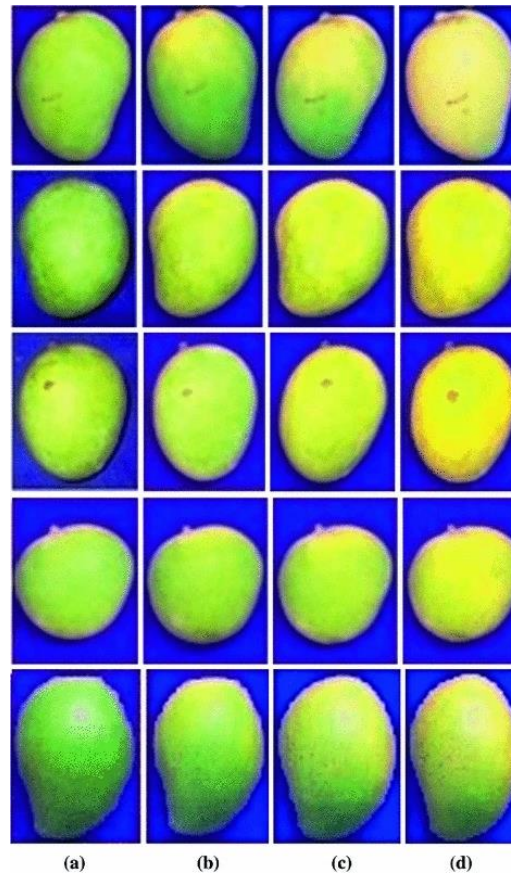


**Figure 2.19.** Five varieties mango with different maturity levels. Each row represented a different variety and each column (a) to (d) representing different maturity as M1, M2, M3, and M4 respectively (figure source Nandi et al. 2014).

The color classification was done using Gaussian Mixture Model which calculates differences of average R, G, and B values of the entire mango. Estimation of these parameters was used to predict the maturity level. The size of the mango is estimated by quantifying the number of pixels that cover the fruit image and the size estimated. The fruits are categorized as small, medium, big, and very big depending on the number of pixels of the binary image of the mango. Finally, fuzzy logic techniques were used to sort and grade the mango fruit. The classification accuracy compared for the system and the average of three experts for five varieties of mango had almost identical results.

## Summary

Image analysis paired with machine learning provides versatility and robustness when compared with manual visual evaluation. For RGB leaf damage images, image analysis using color threshold, segmentation, and binary methods are useful to evaluate symptoms such as chlorosis, necrosis, leaf deformation, and mosaics. Multispectral and hyperspectral imaging based on reflectance are good for early detection, identification and separating different diseases. Plant stress displayed in distinct color can be easily analyzed using RGB imaging but certain stresses such as water or salt are better using thermal or spectral imaging. Plant growth generally is evaluated based on the green reflectance using RGB imaging or measured by hand-held spectroradiometer that measures NDVI. Counting insects or plants depends on machine learning to identify specific features using classification algorithms such as convolutional neural network and support vector machine. Algorithms are able to mimic how humans learn and classify objects. However, mistakes can still occur if object features are difficult to detect, two objects overlapped, or only part of the object is detected. Quality and size evaluation is the hardest to do in the field and is mostly applied in commercial sorting lines. Two examples on production line methods were explored using RGB imaging combined with machine learning for classification on defects and sizes. Case studies in this chapter showed image analysis is more advantageous than visual rating. The advantageous of these methods include objectivity, speed when automated, and more reproducible and reliable results. With the advancement in cameras, computers with high computing power, and the development of different algorithms, image analysis and machine learning

have the potential to replace part of the labor and improve the current data collection procedures in agricultural research.

## References

- Agehara S (2020) Simple Imaging Techniques for Plant Growth Assessment. *EDIS* 2020:5
- Ali R, Abbas H (2003) Response of salt stressed barley seedlings to phenylurea. *Plant, Soil and Environment* v.49 no.4 pp. 158-162
- Apan A, Held A, Phinn S, Markley J (2004) Detecting sugarcane ‘orange rust’ disease using EO-1 Hyperion hyperspectral imagery. *Int J Remote Sens* 25:489–498
- Aparicio N, Villegas D, Casadesus J, Araus JL, Royo C (2000) Spectral Vegetation Indices as Nondestructive Tools for Determining Durum Wheat Yield. *Agron J* 92:83–91
- ARJENAKI O, MOGHADDAM P, MOTLAGH A (2013) Online tomato sorting based on shape, maturity, size, and surface defects using machine vision. *Turk J Agric For* 37:62–68
- Barbosa GL, Gadelha FDA, Kublik N, Proctor A, Reichelm L, Weissinger E, Wohlleb GM, Halden RU (2015) Comparison of Land, Water, and Energy Requirements of Lettuce Grown Using Hydroponic vs. Conventional Agricultural Methods. *Int J Environ Res Public Health* 12:6879–6891
- Bauer S, Wiest R, Nolte L-P, Reyes M (2013) A survey of MRI-based medical image analysis for brain tumor studies. *Phys Med Biol* 58:R97
- Belanger MJ, Miller JR, Boyer MG (1995) Comparative Relationships between Some Red Edge Parameters and Seasonal Leaf Chlorophyll Concentrations. *Can J Remote Sens* 21:16–21
- Bhattacharya A, Sood P, Citovsky V (2010) The roles of plant phenolics in defence and communication during *Agrobacterium* and *Rhizobium* infection. *Mol Plant Pathol* 11:705–719
- Bock CH, Barbedo JGA, Del Ponte EM, Bohnenkamp D, Mahlein A-K (2020) From visual estimates to fully automated sensor-based measurements of plant disease severity: status and challenges for improving accuracy. *Phytopathol Res* 2:9
- Bock CH, Parker PE, Cook AZ, Riley T, Gottwald TR (2009) Comparison of Assessment of Citrus Canker Foliar Symptoms by Experienced and Inexperienced Raters. *Plant Dis* 93:412–424
- Booth DT, Cox SE, Berryman RD (2006) Point Sampling Digital Imagery with ‘Samplepoint.’ *Environ Monit Assess* 123:97–108

- Borges N, Capucho A, Lanna Filho R (2020) A standard area diagram set for assessing severity of eucalyptus bacterial blight caused by *Erwinia psidii*. *Arq Inst Biológico* 87:1–4
- Boyer JS (1982) Plant Productivity and Environment. *Science* 218:443–448
- Brugger A, Behmann J, Paulus S, Luigs H-G, Kuska MT, Schramowski P, Kersting K, Steiner U, Mahlein A-K (2019) Extending Hyperspectral Imaging for Plant Phenotyping to the UV-Range. *Remote Sens* 11:1401
- Cabrera-Bosquet L, Molero G, Stellacci A, Bort J, Nogués S, Araus J (2011) NDVI as a potential tool for predicting biomass, plant nitrogen content and growth in wheat genotypes subjected to different water and nitrogen conditions. *Cereal Res Commun* 39:147–159
- Camargo A, Smith JS (2009) An image-processing based algorithm to automatically identify plant disease visual symptoms. *Biosyst Eng* 102:9–21
- Carter GA, Knapp AK (2001) Leaf optical properties in higher plants: linking spectral characteristics to stress and chlorophyll concentration. *Am J Bot* 88:677–684
- Casari RACN, Paiva DS, Silva VNB, Ferreira TMM, Souza J, Oliveira NG, Kobayashi AK, Molinari HBC, Santos TT, Gomide RL, Magalhães PC, Sousa CAF (2019) Using Thermography to Confirm Genotypic Variation for Drought Response in Maize. *Int J Mol Sci* 20:2273
- Chaimala A, Jogloy S, Vorasoot N, Toomsan B, Jongrungklang N, Kesmala T, Holbrook CC, Kvien CK (2020) Responses of Total Biomass, Shoot Dry Weight, Yield and Yield Components of Jerusalem Artichoke (*Helianthus tuberosus* L.) Varieties under Different Terminal Drought Duration. *Agriculture* 10:198
- Chen D, Brutsaert W (1998) Satellite-Sensed Distribution and Spatial Patterns of Vegetation Parameters over a Tallgrass Prairie. *J Atmospheric Sci* 55:1225–1238
- Chen J, Fan Y, Wang T, Zhang C, Qiu Z, He Y (2018) Automatic Segmentation and Counting of Aphid Nymphs on Leaves Using Convolutional Neural Networks. *Agronomy* 8:129
- Chen L, Zhang J-G, Su H-F, Guo W (2010) Weed identification method based on probabilistic neural network in the corn seedlings field. Pages 1528–1531 in 2010 International Conference on Machine Learning and Cybernetics
- Chen X (2021) Effects of micro-rates of 2, 4-D and dicamba on lettuce and pumpkin in Nebraska. M.S. dissertation. Lincoln: University of Nebraska. 180 p
- Chen Y-R, Chao K, Kim MS (2002) Machine vision technology for agricultural applications. *Comput Electron Agric* 36:173–191

- Choi J, Cha D, Kim D-S, Lee S (2019) Review of Japanese Pine Bast Scale, *Matsucoccus matsumurae* (Kuwana) (Cocomorpha: Matsucoccidae), Occurring on Japanese Black Pine (*Pinus thunbergii* Parl.) and Japanese Red Pine (*P. densiflora* Siebold & Zucc.) from Korea. *Forests* 10:639
- Contreras-Medina LM, Osornio-Rios RA, Torres-Pacheco I, Romero-Troncoso R de J, Guevara-González RG, Millan-Almaraz JR (2012) Smart Sensor for Real-Time Quantification of Common Symptoms Present in Unhealthy Plants. *Sensors* 12:784–805
- Datt B, McVicar TR, Van Niel TG, Jupp DLB, Pearlman JS (2003) Preprocessing EO-1 Hyperion hyperspectral data to support the application of agricultural indexes. *IEEE Trans Geosci Remote Sens* 41:1246–1259
- Domiciano G, Duarte H, Moreira E, Rodrigues F (2013) Development and validation of a set of standard area diagrams to aid in estimation of spot blotch severity on wheat leaves. *Plant Pathol* 63
- Dougherty G (2009) *Digital Image Processing for Medical Applications*. Cambridge University Press. 463 p
- Duan J, Zhao B, Wang Y, Yang W (2015) Development and validation of a standard area diagram set to aid estimation of bacterial spot severity on tomato leaves. *Eur J Plant Pathol* 142:665–675
- ElMasry G, Cubero S, Moltó E, Blasco J (2012) In-line sorting of irregular potatoes by using automated computer-based machine vision system. *J Food Eng* 112:60–68
- Franceschi VT, Alves KS, Mazaro SM, Godoy CV, Duarte HSS, Del Ponte EM (2020) A new standard area diagram set for assessment of severity of soybean rust improves accuracy of estimates and optimizes resource use. *Plant Pathol* 69:495–505
- Garbulsky MF, Peñuelas J, Gamon J, Inoue Y, Filella I (2011) The photochemical reflectance index (PRI) and the remote sensing of leaf, canopy and ecosystem radiation use efficiencies: A review and meta-analysis. *Remote Sens Environ* 115:281–297
- Garg PK (2020) 10 - Effect of contamination and adjacency factors on snow using spectroradiometer and hyperspectral images. Pages 167–196 in PC Pandey, PK Srivastava, H Balzter, B Bhattacharya, GP Petropoulos, eds. *Hyperspectral Remote Sensing*. Elsevier
- Gaspar T, Franck T, Bisbis B, Kevers C, Jouve L, Hausman JF, Dommes J (2002) Concepts in plant stress physiology. Application to plant tissue cultures. *Plant Growth Regul* 37:263–285

- Gitelson AA, Zur Y, Chivkunova OB, Merzlyak MN (2002) Assessing Carotenoid Content in Plant Leaves with Reflectance Spectroscopy. *Photochem Photobiol* 75:272–281
- Giusti MM, Polit MF, Ayvaz H, Tay D, Manrique I (2014) Characterization and Quantitation of Anthocyanins and Other Phenolics in Native Andean Potatoes. *J Agric Food Chem* 62:4408–4416
- Govaerts B, Verhulst N (2010) The normalized difference vegetation index (NDVI) Greenseeker(TM) handheld sensor: toward the integrated evaluation of crop management. Part A - Concepts and case studies. CIMMYT
- Hagemeyer J (2004) Ecophysiology of Plant Growth Under Heavy Metal Stress. Pages 201–222 *in* MNV Prasad, ed. *Heavy Metal Stress in Plants: From Biomolecules to Ecosystems*. Berlin, Heidelberg: Springer
- He K, Gkioxari G, Dollar P, Girshick R (2017) Mask R-CNN. Pages 2961–2969 *in*
- Heiberg E, Sjögren J, Ugander M, Carlsson M, Engblom H, Arheden H (2010) Design and validation of Segment - freely available software for cardiovascular image analysis. *BMC Med Imaging* 10:1
- Hodgson EW, McCornack BP, Tilmon K, Knodel JJ (2012) Management Recommendations for Soybean Aphid (Hemiptera: Aphididae) in the United States. *J Integr Pest Manag* 3:E1–E10
- Hong S-J, Nam I, Kim S-Y, Kim E, Lee C-H, Ahn S, Park I-K, Kim G (2021) Automatic Pest Counting from Pheromone Trap Images Using Deep Learning Object Detectors for *Matsucoccus thunbergianae* Monitoring. *Insects* 12:342
- Jacquemoud S, Ustin SL (2001) Leaf optical properties: A state of the art. Pages 223–332 *in* *8th International Symposium of Physical Measurements & Signatures in Remote Sensing*
- Jain S, Patil B (2014) Cancer Cells Detection Using Digital Image Processing Methods. *Int J Latest Res Sci Technol VOLUME* 3:45–49
- James WC (1971) illustrated series of assessment keys for plant diseases, their preparation and usage. *Can Plant Dis Surv*, 51: 39–65.
- Jarimopas B, Jaisin N (2008) An experimental machine vision system for sorting sweet tamarind. *J Food Eng* 89:291–297
- Jermi M, Blaise P, C. G (2010) Quantitative effect of leaf damage caused by downy mildew (*Plasmopara viticola*) on growth and yield quality of grapevine “Merlot” (*Vitis vinifera*). *Vitis -Geilweilerhof-* 79:77–85

- Jeyalakshmi S, Radha R (2017) A review on diagnosis of nutrient deficiency symptoms in plant leaf image using digital image processing. *ICTACT J Image Video Process* 7:1515–1524
- Ji L, Peters AJ (2003) Assessing vegetation response to drought in the northern Great Plains using vegetation and drought indices. *Remote Sens Environ* 87:85–98
- Johnson KD, O’Neal ME, Ragsdale DW, Difonzo CD, Swinton SM, Dixon PM, Potter BD, Hodgson EW, Costamagna AC (2009) Probability of Cost-Effective Management of Soybean Aphid (Hemiptera: Aphididae) in North America. *J Econ Entomol* 102:2101–2108
- Keshava N, Mustard JF (2002) Spectral unmixing. *IEEE Signal Process Mag* 19:44–57
- Khaki S, Pham H, Khalilzadeh Z, Masoud A, Safaei N, Han Y, Kent W, Wang L (2022) High-throughput image-based plant stand count estimation using convolutional neural networks. *PLOS ONE* 17:e0268762
- Komarkova J, Jech J, Sedlak P (2020) Comparison of Vegetation Spectral Indices Based on UAV Data : Land Cover Identification Near Small Water Bodies. Pages 1–4 *in* 2020 15th Iberian Conference on Information Systems and Technologies (CISTI)
- Krizhevsky A, Sutskever I, Hinton GE (2017) ImageNet classification with deep convolutional neural networks. *Commun ACM* 60:84–90
- Lara MÁ, Diezma B, Lleó L, Roger JM, Garrido Y, Gil MI, Ruiz-Altisent M (2016) Hyperspectral Imaging to Evaluate the Effect of Irrigation Water Salinity in Lettuce. *Appl Sci* 6:412
- Larrinaga AR, Brotons L (2019) Greenness Indices from a Low-Cost UAV Imagery as Tools for Monitoring Post-Fire Forest Recovery. *Drones* 3:6
- Läuchli A, Grattan SR (2007) Plant Growth And Development Under Salinity Stress. Pages 1–32 *in* MA Jenks, PM Hasegawa, SM Jain, eds. *Advances in Molecular Breeding Toward Drought and Salt Tolerant Crops*. Dordrecht: Springer Netherlands
- Lee D-J, Archibald JK, Xiong G (2011) Rapid Color Grading for Fruit Quality Evaluation Using Direct Color Mapping. *IEEE Trans Autom Sci Eng* 8:292–302
- Li C, Adhikari R, Yao Y, Miller AG, Kalbaugh K, Li D, Nemali K (2020) Measuring plant growth characteristics using smartphone based image analysis technique in controlled environment agriculture. *Comput Electron Agric* 168:105123
- Li Q, Wang M, Gu W (2002) Computer vision based system for apple surface defect detection. *Comput Electron Agric* 36:215–223

- Liang L, Schwartz MD, Fei S (2012) Photographic assessment of temperate forest understory phenology in relation to springtime meteorological drivers. *Int J Biometeorol* 56:343–355
- Lowe A, Harrison N, French AP (2017) Hyperspectral image analysis techniques for the detection and classification of the early onset of plant disease and stress. *Plant Methods* 13:80
- Mahlein A-K (2016) Plant Disease Detection by Imaging Sensors – Parallels and Specific Demands for Precision Agriculture and Plant Phenotyping. *Plant Dis* 100:241–251
- Mahlein A-K, Kuska MT, Behmann J, Polder G, Walter A (2018) Hyperspectral Sensors and Imaging Technologies in Phytopathology: State of the Art. *Annu Rev Phytopathol* 56:535–558
- Naik HS, Zhang J, Lofquist A, Assefa T, Sarkar S, Ackerman D, Singh A, Singh AK, Ganapathysubramanian B (2017) A real-time phenotyping framework using machine learning for plant stress severity rating in soybean. *Plant Methods* 13:23
- Nandi CS, Tudu B, Koley C (2014) Machine Vision Based Techniques for Automatic Mango Fruit Sorting and Grading Based on Maturity Level and Size. Pages 27–46 in A Mason, SC Mukhopadhyay, KP Jayasundera, N Bhattacharyya, eds. *Sensing Technology: Current Status and Future Trends II*. Cham: Springer International Publishing
- Nutter FWJ, Gleason ML, Jenco JH, Christians NC (1993) Assessing the accuracy, intra-rater repeatability, and inter-rater reliability of disease assessment systems. *Phytopathol USA*
- Paruelo JM, Lauenroth WK, Roset PA (2000) Estimating Aboveground Plant Biomass Using a Photographic Technique. *J Range Manag* 53:190–193
- Pathak H, Igathinathane C, Zhang Z, Archer D, Hendrickson J (2022) A review of unmanned aerial vehicle-based methods for plant stand count evaluation in row crops. *Comput Electron Agric* 198:107064
- Patrignani A, Ochsner TE (2015) Canopeo: A Powerful New Tool for Measuring Fractional Green Canopy Cover. *Agron J* 107:2312–2320
- Pratt WK (2001) *Digital Image Processing*. New York, USA: John Wiley & Sons, Inc.
- Rafiq A, Makroo HA, Hazarika MK (2016) Artificial Neural Network-Based Image Analysis for Evaluation of Quality Attributes of Agricultural Produce. *J Food Process Preserv* 40:1010–1019

- Richardson AD, Jenkins JP, Braswell BH, Hollinger DY, Ollinger SV, Smith M-L (2007) Use of digital webcam images to track spring green-up in a deciduous broadleaf forest. *Oecologia* 152:323–334
- Romano G, Zia S, Spreer W, Sanchez C, Cairns J, Araus JL, Müller J (2011) Use of thermography for high throughput phenotyping of tropical maize adaptation in water stress. *Comput Electron Agric* 79:67–74
- Römer C, Wahabzada M, Ballvora A, Pinto F, Rossini M, Panigada C, Behmann J, León J, Thureau C, Bauckhage C, Kersting K, Rascher U, Plümer L (2012) Early drought stress detection in cereals: simplex volume maximisation for hyperspectral image analysis. *Funct Plant Biol* 39:878–890
- Rumpf T, Mahlein A-K, Steiner U, Oerke E-C, Dehne H-W, Plümer L (2010) Early detection and classification of plant diseases with Support Vector Machines based on hyperspectral reflectance. *Comput Electron Agric* 74:91–99
- Sahitya A, Nadar I, Sakhiya P, Mishra A (2021) Quality Analysis on Agricultural Produce Using CNN. SSRN Scholarly Paper. Rochester, NY
- Sarkar S, Ramsey AF, Cazenave A-B, Balota M (2021) Peanut Leaf Wilting Estimation From RGB Color Indices and Logistic Models. *Front Plant Sci* 12
- Shajahan S (2019) Agricultural Field Applications of Digital Image Processing Using an Open Source ImageJ Platform, North Dakota State University
- Shajahan S, Sivarajan S, Maharlooei M, Bajwa SG, Harmon JP, Nowatzki JF, Cannayen I (2017) Identification and Counting of Soybean Aphids from Digital Images Using Shape Classification. *Trans ASABE* 60:1467–1477
- Shi C, Wang L (2014) Incorporating spatial information in spectral unmixing: A review. *Remote Sens Environ* 149:70–87
- Shimizu H, Saito Y, Nakashima H, Miyasaka J, Ohdoi K (2011) Light Environment Optimization for Lettuce Growth in Plant Factory. *IFAC Proc Vol* 44:605–609
- Shirzadifar A, Maharlooei M, Bajwa SG, Oduor PG, Nowatzki JF (2020) Mapping crop stand count and planting uniformity using high resolution imagery in a maize crop. *Biosyst Eng* 200:377–390
- Simonyan K, Zisserman A (2015) Very Deep Convolutional Networks for Large-Scale Image Recognition. *arXiv preprint arXiv:1409.1556*
- Singh V, Sharma N, Singh S (2020) A review of imaging techniques for plant disease detection. *Artif Intell Agric* 4:229–242
- Skirycz A, Inzé D (2010) More from less: plant growth under limited water. *Curr Opin Biotechnol* 21:197–203

- Sotiropoulos TE, Therios IN, Dimassi KN, Bosabalidis A, Kofidis G (2002) Nutritional Status, Growth, Co<sub>2</sub> Assimilation, and Leaf Anatomical Responses in Two Kiwifruit Species Under Boron Toxicity. *J Plant Nutr* 25:1249–1261
- Stewart AM, Edmisten KL, Wells R, Collins GD (2007) Measuring Canopy Coverage with Digital Imaging. *Commun Soil Sci Plant Anal* 38:895–902
- Stewart EL, McDonald BA (2014) Measuring Quantitative Virulence in the Wheat Pathogen *Zymoseptoria tritici* Using High-Throughput Automated Image Analysis. *Phytopathology*® 104:985–992
- Sytar O, Brestic M, Zivcak M, Olsovska K, Kovar M, Shao H, He X (2017) Applying hyperspectral imaging to explore natural plant diversity towards improving salt stress tolerance. *Sci Total Environ* 578:90–99
- Taiz L, Zeiger E, Møller IM, Murphy A (2015) *Plant physiology and development*. Sunderland, MA: Sinauer Associates. ISBN : 9781605353531
- Thurau C, Kersting K, Bauckhage C (2010) Yes we can: simplex volume maximization for descriptive web-scale matrix factorization. Pages 1785–1788 *in* Proceedings of the 19th ACM international conference on Information and knowledge management. New York, NY, USA: Association for Computing Machinery
- Ungar SG (2001) Overview of EO-1, the first 120 days. Pages 43–45 volume1 *in* IGARSS 2001. Scanning the Present and Resolving the Future. Proceedings. IEEE 2001 International Geoscience and Remote Sensing Symposium (Cat. No.01CH37217)
- Vapnik VN (1998) *Statistical Learning Theory* 1st edition. New York: Wiley-Interscience. 768 p
- Wahabzada M, Mahlein A-K, Bauckhage C, Steiner U, Oerke E-C, Kersting K (2015) Metro Maps of Plant Disease Dynamics—Automated Mining of Differences Using Hyperspectral Images. *PLOS ONE* 10:e0116902
- Xu HR, Ying YB, Fu XP, Zhu SP (2007) Near-infrared Spectroscopy in detecting Leaf Miner Damage on Tomato Leaf. *Biosyst Eng* 96:447–454
- Yang J, Yen HE (2002) Early Salt Stress Effects on the Changes in Chemical Composition in Leaves of Ice Plant and Arabidopsis. A Fourier Transform Infrared Spectroscopy Study. *Plant Physiol* 130:1032–1042
- Zandalinas SI, Fritschi FB, Mittler R (2021) Global Warming, Climate Change, and Environmental Pollution: Recipe for a Multifactorial Stress Combination Disaster. *Trends Plant Sci* 26:588–599
- Zhao Y, Gong L, Huang Y, Liu C (2016) A review of key techniques of vision-based control for harvesting robot. *Comput Electron Agric* 127:311–323

Zia S, Romano G, Spreer W, Sanchez C, Cairns J, Araus JL, Müller J (2013) Infrared Thermal Imaging as a Rapid Tool for Identifying Water-Stress Tolerant Maize Genotypes of Different Phenology. *J Agron Crop Sci* 199:75–84

## Chapter 3: Machine learning grading for lettuce bolting and compactness

### Introduction

Lettuce (*Lactuca sativa* L.) is a major fresh vegetable and is commonly used in salad mixtures and sandwiches. The United States has the largest production of lettuce as a salad crop, and produced 22% of the world's lettuce supply (Mou 2008). Yuma County, Arizona is known as the "Lettuce Capital of the World" or "Winter Salad Bowl" for its renowned winter-grown lettuce from November through March. Arizona State University lists the three major lettuce types growing in Yuma County are iceberg, romaine, and baby leaf. In 2010, lettuce production included approximately 50,000 acres of iceberg followed by approximately 30,000 acres of romaine varieties, and approximately 25,000 acres of baby leaf varieties (USDA, National Agricultural Statistics Service, Arizona). The winter lettuce production in Arizona was worth about \$321 million (USDA, National Agricultural Statistics Service, Arizona).

Research Designed for Agriculture (RD4AG) is a commercial contracted agriculture research company located in Yuma, Arizona. Romaine lettuce has been widely used at RD4AG to test the efficacy of growth stimulators together with reduced rates of fertilizers. The important quality factors for data collection in romaine are compactness and bolting. Compactness is the measurement of the internal density of the head that is closely related to shelf life. More compact lettuce has better quality and longer shelf life compared with less compacted ones. Bolting is another quality feature measured in romaine that measures the future flower stalk at the "butt" end of the head. Bolted lettuce is unmarketable due to its bitter taste. At RD4AG, both measurements are done by slicing the lettuce through the middle and looking at the inner features. For

compactness, a 1-5 rating scale is based on the heart and leaf tightness. The five levels are: 1) very immature, just heading, the center is open; 2) leaves in center are smaller and the head is open; 3) starting to mature but leaves on top are mostly open and individually identifiable; 4) fully mature and commercially desirable, head is weighty and full; and 5) overmature, leaves at the top are pushing way out of the head (Figure 3.1). For the 1-5 bolting rating, the shape and length of the “butt” end of the head are the main identification features. The five levels are: 1) not bolting— butt rounded and an inch or less in length; 2) older—round, butt 1.5-2 inches in length; 3) starting to bolt, butt is starting to point and the pointed butt is 1.5-2 inches in length; 4) continue bolting and the pointed butt is 2 or 3 inches long and elongating; and 5) not marketable— pointed butt is 3.5 inches long and obviously bolting (Figure 3.2). In commercial grading, compactness rating at 3 and 4 are marketable where bolting rating at 1 to 3 are considered marketable.

Imaging is adopted at RD4AG by taking images of the sliced lettuce heads in the field by using a photo cart. Typically, 10 lettuce heads are included for each plot to ensure representative sampling. Images are saved for later evaluation by trained and experienced raters. However, this grading process is laborious and time-consuming. Training and testing people on grading requires time to ensure accuracy. This is important because grading for either compactness or bolting has five levels and the middle levels from two to four share similarities that can be hard to distinguish.

Convolutional neural networks (CNN) are complex models used for machine learning and classification. The neural networks can increase the probability of correct classifications with adequately large data sets of images (i.e., hundreds to thousands of measurements, depending on the complexity of the problem under study) for training

(Kamilaris and Prenafeta-Boldú 2018). CNN consists of input, convolutional, pooling, and fully connected layers (O'Shea and Nash 2015). The input layer will hold the pixel values of the image. The convolutional layer contains a set of filters that are used for feature extraction. This layer deals with the spatial redundancy by weight sharing. Weight sharing is a way to reduce the number of parameters while allowing for more robust feature detection. During the training process, the spatial redundancy is reduced and features will become more exclusive and informative (Santosh et al. 2022). The pooling layer will reduce the dimension of the input images by combining those spatial redundancies as specific features and move to the next layer (Djordjevic 2021). The pooling process is important in reducing the processing speed. Fully connected is the last layer that takes in the feature information from the previous layers and assigns weights to predict the correct label (Basha et al. 2020, Schmidhuber 2015). CNN has been used in multiple areas in agriculture. Kussul et al. (2017) used CNN for crop type classification that had 94.6% accuracy to classify the crop type of wheat, maize, soybean, sunflower, and sugar beet. Xinshao and Cheng (2015) used 3980 images that contained 91 types of weed seeds for training, and the trained model was able to classify them individually at 90.96% accuracy. CNN techniques were used in fruit counting by multiple researchers including Rahnemoonfar and Sheppard (2017) to predict the number of tomatoes in images. Chen et al. (2017) used CNN to count the number of apples and oranges in images, and Sa et al. (2016) for identify and counting of sweet peppers and melons.

Thus, a potential solution using CNN image machine learning will be explored in this chapter. Two individual Convolution2D models will be separately trained for grading bolting and compactness of romaine lettuce heads. The objective is to test the accuracy of

each trained model and explore if the model can potentially replace visual grading typically done by professionals.

### **Materials and Method**

Images used for romaine lettuce machine learning were acquired at RD4AG. These images were taken in the field using a mobile cart with a camera mounted on top. For each image, 10 heads of lettuce from the same plot were laid in a 2×5 grid. Each lettuce head had been graded for compactness and bolting, and those data were used as labeled data for training the model. Because there are 10 heads of lettuce included in each image, each lettuce head needed to be cropped out as an image of a single lettuce head. However, due to differences in the grid layouts and overlap of leaves between heads across different trials or images, it was often difficult to obtain uniform images of the various heads.

Images of individual lettuce heads were manually cropped using the screenshot function on the laptop. After that, each cropped lettuce image was standardized at 100×100 pixels. These images were labeled for either compactness or bolting based on the grading assigned by the professionals. Labeling will enable the CNN model to recognize each image in the training process.

For each level from one to five, 20 images were used for training, and an extra five images were held out to be used for validation. However, through four trials of over 4000 lettuce heads, only three heads were found that rated 1's for bolting or compactness. Of these, two heads were used for training and one for validation. Bolting ratings of 5's included only six lettuce heads; thus, three heads were used for training and three heads for validation. The training images were fed into the CNN algorithm for training, and a

specialized model for either bolting or compactness prediction was acquired. Convolution2D was used for training, and based on training images, different layers for feature extraction were created. Feature extraction from an image included the processes of convolutional, pooling, and fully connected. After the identification model was developed, validation images were input into each model to determine the accuracy of prediction. The model established a rating prediction for each head that was expressed as the probability for each rating. Thus, the highest probability rating was determined to be its predicted rating.

### **Results and Discussion**

The prediction model for compactness showed total accuracy for the validation group of 66.6% (14/21) (Table 3.1). Mistakes were observed in prediction for 1-, 2-, and 4-ratings. The prediction for 1-rating was wrong, likely due to only having 2 images for training and 1 for validation. There were errors in the prediction for 2-ratings likely because features extracted were not representative and can be mistaken for other levels that share similar features. In addition, the four false classifications for 4-ratings were likely due to similar features between 4- and 5-ratings. The prediction model for bolting showed total accuracy for the validation group of 68.4% (13/19) (Table 3.2). All prediction errors were observed in grading for 3-, 4-, and 5-ratings. The errors in prediction were likely due to the similarities shared among the three closely related levels.

The accuracy was based on the number of correct predictions out of the total. The CNN model made predictions based on the probability for that rating. Since there were five levels for each quality measurement (compactness or bolting), by random chance,

there would be a 20% chance for each of the five ratings. However, even after the model training, the probability for any rating among the five levels was still not significantly higher than 20% with the highest being approximately 24%. Although the accuracy looks moderate, approaching 70%, for each model, the range of probabilities to support a prediction is not adequate.

Issues related to low accuracy could be because the number of images used for training was not enough and the feature information across the various ratings was inadequate. Many more images will be needed for training the features used to classify the different rating levels to make predictions. From our preliminary model, we suggest having at least a hundred training images at each rating level. The quality of several images had variable shading which also resulted in poor feature extraction. For both compactness and bolting training, there were very limited images representing either 1 or 5. Acquiring those images could improve the accuracy and the range of predictions of all levels. Purposely harvesting lettuce early or late can help acquire those images. In addition, the images used for this training model were not intended for image analysis, and the lighting and grid for placing lettuce heads varied. Cropping lettuce was extremely difficult using the automatic cropping software because of the varied grids. Manual cropping of lettuce heads using screenshots is also not ideal and reduced the quality of the images. We also observed debris, overlapping lettuce leaves, and soil particles on the images which all could contribute to the inaccuracy in the prediction models. Lastly, an accurate rating matched with the corresponding image is crucial. Poor accuracy by the rater could result in inaccuracy used in training models. Cross checking the rating among the raters could reduce the inaccuracies.

In summary, there is huge potential in using machine learning to automatically grade lettuce bolting and compactness. However, placing heads on a consistent grid, regularly cleaning for debris, and avoiding lettuce overlay could help improve the lettuce image quality for more effective cropping and training. Cross-checking the training data among raters could also improve the model accuracy. In addition, the development of a reasonable model will require many more images for compactness and bolting training at all rating levels, but especially at 1 and 5 levels.



**Figure 3.1.** Five levels rating for compactness with three representative lettuce heads for each level (a) compactness of 1; (b) compactness of 2; (c) compactness of 3; (d) compactness of 4; and (e) compactness of 5 (figure credit: RD4AG).



**Figure 3.2.** Five levels rating for bolting with three representative lettuce heads for each level (a) bolting of 1; (b) bolting of 2; (c) bolting of 3; (d) bolting of 4; and (e) bolting of 5 (figure credit: RD4AG).

**Table 3.1.** Validation images for compactness model prediction.

Number of compactness tested	Number of correct estimates	Chance of correct prediction
1	Wrong	0/1
2	Correct	3/5
	Correct	
	Correct	
	Wrong	
	Wrong	
3	Correct	5/5
	Correct	
4	Correct	1/5
	Wrong	
5	Correct	5/5
	Correct	
Total accuracy		14/21

**Table 3.2.** Validation images for bolting model prediction.

Number of bolting tested	Number of correct estimates	Chance of correct prediction
1	Correct	1/1
2	Correct	5/5
	Correct	
	Correct	
	Correct	
3	Correct	3/5
	Correct	
	Correct	
	Wrong	
4	Wrong	2/5
	Wrong	
5	Wrong	2/3
	Wrong	
	Wrong	
Total accuracy		13/19

## References

- Basha SHS, Dubey SR, Pulabaigari V, Mukherjee S (2020) Impact of fully connected layers on performance of convolutional neural networks for image classification. *Neurocomputing* 378:112–119
- Chen SW, Shivakumar SS, Dcunha S, Das J, Okon E, Qu C, Taylor CJ, Kumar V (2017) Counting Apples and Oranges With Deep Learning: A Data-Driven Approach. *IEEE Robot Autom Lett* 2:781–788
- Djordjevic IB (2021) Chapter 14 - Quantum Machine Learning. Pages 619–701 *in* IB Djordjevic, ed. *Quantum Information Processing, Quantum Computing, and Quantum Error Correction (Second Edition)*. Academic Press
- Kamilaris A, Prenafeta-Boldú FX (2018) A review of the use of convolutional neural networks in agriculture. *J Agric Sci* 156:312–322
- Kussul N, Lavreniuk M, Skakun S, Shelestov A (2017) Deep Learning Classification of Land Cover and Crop Types Using Remote Sensing Data. *IEEE Geosci Remote Sens Lett* 14:778–782
- Mou B (2008) Lettuce. Pages 75–116 *in* J Prohens, F Nuez, eds. *Vegetables I: Asteraceae, Brassicaceae, Chenopodiaceae, and Cucurbitaceae*. New York, NY: Springer
- O’Shea K, Nash R (2015) An Introduction to Convolutional Neural Networks. arXiv preprint arXiv:1511.08458.
- Rahnemoonfar M, Sheppard C (2017) Deep Count: Fruit Counting Based on Deep Simulated Learning. *Sensors* 17:905
- Sa I, Ge Z, Dayoub F, Upcroft B, Perez T, McCool C (2016) DeepFruits: A Fruit Detection System Using Deep Neural Networks. *Sensors* 16:1222
- Santosh K, Das N, Ghosh S (2022) Chapter 2 - Deep learning: a review. Pages 29–63 *in* K Santosh, N Das, S Ghosh, eds. *Deep Learning Models for Medical Imaging*. Academic Press
- Schmidhuber J (2015) Deep learning in neural networks: An overview. *Neural Netw* 61:85–117
- Xinshao W, Cheng C (2015) Weed seeds classification based on PCANet deep learning baseline. Pages 408–415 *in* 2015 Asia-Pacific Signal and Information Processing Association Annual Summit and Conference (APSIPA)